Title	Simultaneous determination of insoluble fluoride-forming and high field-strength element abundances in rock samples by ICP-QMS through isotope dilution-internal standardisation
Author(s)	Kagami Saya, Yokoyama Tetsuya
Citation	Geostandards and Geoanalytical Research, 45(4), p.679-699
Text Version	Published Journal Article
URL	https://jopss.jaea.go.jp/search/servlet/search?5070207
DOI	https://doi.org/10.1111/ggr.12394
Right	© 2021 The Authors. Geostandards and Geoanalytical Research © 2021 International Association of Geoanalysts.

Vol. 45 — N° 4 12 21 p. 679 – 699

GEOSTANDARDS and GEOANALYTICAL RESEARCH

Simultaneous Determination of Insoluble Fluoride-Forming and High Field-Strength Element Abundances in Rock Samples by ICP-QMS through Isotope Dilution-Internal Standardisation

Saya **Kagami** (1, 2)* and Tetsuya **Yokoyama** (2)

(1) Tono Geoscience Center, Japan Atomic Energy Agency (JAEA), Jorinji, Izumicho, Toki 509-5102, Japan
(2) Department of Earth and Planetary Sciences, Tokyo Institute of Technology, Ookayama, Tokyo 152-8551, Japan
* Corresponding author. e-mail: kagami.saya@jaea.go.jp

A new method for precise measurement of the mass fractions of insoluble fluoride-forming elements (IFFEs) and high field-strength elements (HFSEs) in rock samples by ICP-QMS was developed. Unlike previous methods, in which the two elemental groups are measured separately using two solutions prepared from distinct sample aliquots (i.e., separate methods), this technique prepares a solution by acid digestion from a single sample aliquot, then divides the solution into two fractions that are dedicated to the measurement of IFFEs and HFSEs. The incorporation of IFFEs/HFSEs into insoluble fluorides during HF digestion was overcome by adjusting the Ca-Al-Mg composition of the sample by Al addition before acid digestion. The acceptable composition was Ca/(Ca+Al) $<$ 0.43 and Mg/(Mg+Al) $<$ 0.40 with hot plate digestion, whereas the limited condition of Ca/(Ca+Al) $<$ 0.40, Mg/(Mg+Al) $<$ 0.40 and Al/(Mg+Ca) $<$ 1.86 was required for digestion under high pressure and temperature. For samples with an unacceptable composition, the change in Ca-Al-Mg composition by Mg/Ca addition should be prohibited because the reaction of HF with the added solution before sample decomposition forms fluorides that coprecipitate HFSEs. The developed method yielded mass fractions consistent with data from the separate methods ($\pm$ 5%) and achieved a repeatability of $<$ 4% for most elements.

Keywords: quadrupole ICP-MS, HFSE, trace elements, isotope dilution, internal standardisation, rock samples, Ca-Al-Mg composition.

Received 13 Nov 20 – Accepted 17 May 21

The abundance of trace elements in extra-terrestrial and terrestrial materials provides fundamental information to understanding the origin of the Solar System and the evolutionary histories of asteroids and planets (e.g., Münker *et al.* 2003). In recent geochemistry, the determination of trace element abundances in meteorites, terrestrial rocks and their components has been usually conducted using solution-based inductively coupled plasma-mass spectrometry (ICP-MS) and laser ablation ICP-MS (LA-ICP-MS) (e.g., Barrat *et al.* 2007). The LA-ICP-MS technique has the advantage of spatial resolution, which enables spot and in situ analyses on a scale of a few tens of μm. However, the measurement precision is approximately 10% of the relative standard deviation (RSD) for most cases (e.g., Pearce *et al.* 2011). In addition, the use of matrix-matched measurement standards is favoured to achieve accurate results in LA-ICP-MS (e.g., Jochum *et al.* 2007). In contrast, measurements with solution-based ICP-MS provide accurate data for trace element abundances with precision of $<$ 5% of the RSD when a sufficient signal intensity is obtained, although the spatial information is minimised. In solution-based ICP-MS, the influence of the matrix effect can be reduced either by adding an internal standard and diluting the sample solution by acid with a large dilution factor (i.e., internal standardisation), or by adding spikes and separating the target elements with ion-exchange chromatography (i.e., isotope dilution) (e.g., Heumann 2004, Yokoyama *et al.* 2017).

To determine the mass fraction of the measurand in rock samples by solution-based ICP-MS, rock samples digested either by alkali fusion or by acid attack must be dissolved into a solution. The alkali fusion method facilitates complete dissolution of acid-resistant minerals such as zircon and spinel but is hampered by the contamination of alkaline trace elements (Eggins 2003). On the other hand, the acid digestion method generally uses HF to decompose silicate minerals. Makishima

doi: 10.1111/ggr.12394

et al. (2009) proposed a new classification of elements by which elements in the periodic table are divided into seven groups based on the chemical behaviour of the individual elements in an HF solution. Of the seven groups, insoluble fluoride-forming elements (IFFEs) include alkaline earth metals, lanthanoids and Th, all of which coprecipitate with fluorides such as MgF_2, $CaAlF_5$ and ralstonite ($Na_{0.88}Mg_{0.88}Al_{1.12}(F, OH)_6{\cdot}H_2O$) if fluoride ions are present in the solution (Yokoyama *et al.* 1999). In contrast, high field-strength elements (HFSEs: Ti, Zr, Nb, Hf and Ta) belong to the 'fluorophile elements', which form stable soluble fluoro-complexes in HF. Therefore, it has been argued that IFFEs and HFSEs cannot be dissolved in the same solution on digesting a rock sample using HF, which makes it difficult for the solution-based ICP-MS to simultaneously measure these elements in a single aliquot of a rock sample. Considering the difference in chemical characteristics between two groups IFFEs and HFSEs, two aliquots of powders from a single rock sample are weighed and then dissolved separately through different digestion methods for the measurements of IFFEs and HFSEs. Such a method is called the 'separate method' hereafter. Alternatively, simultaneous determination of IFFEs and HFSEs is hereafter called the 'simultaneous method'. Many previous studies perform the simultaneous method by dissolving a single aliquot of a rock sample in a mixture of HNO_3 and trace HF after the digestion of soluble fluorides by $HClO_4$ (e.g., Senda *et al.* 2014). In practice, this method can form fluorides because a final solution contains HF. Cotta and Enzweiler (2012) analysed samples in an HNO_3 solution after fluoride digestion by $HClO_4$. In this case, HFSEs can precipitate as oxides (Yokoyama *et al.* 1999). Moreover, a dissolved sample in an HNO_3 solution was measured by ICP-MS after digestion by HNO_3 and HF without $HClO_4$ (e.g., Eggins *et al.* 1997, Liang *et al.* 2000, Liang and Grégoire 2000, Hu and Gao 2008), which means the HFSE fluoride cannot be completely digested. In most cases, the biases in the mass fractions measured by this method are within approximately 10% compared with the literature data. Therefore, these simultaneous methods that have been reported previously risk the incomplete recovery of either IFFEs or HFSEs owing to their different chemical characteristics mentioned above.

Another potential problem that occurs during the determination of HFSEs by solution-based ICP-MS is the coprecipitation of some HFSEs with insoluble fluorides of which the precipitation rate strongly depends on the composition of major elements (Ca, Al and Mg) in rock samples (Tanaka *et al.* 2003). The authors argued that incomplete recovery of Zr, Nb, Hf and Ta owing to coprecipitation with insoluble fluorides occurs for a Ca-rich sample when the molar ratio of Ca/(Ca+Al), denoted as Ca# in this study, in the sample solution (0.5 mol l^{-1} HF) was > 0.40. On the other hand, the formation of insoluble AlF_3 that incorporates some IFFEs in the structure, specifically for rare earth elements (REEs), occurs when a rock sample with a high Al/(Mg+Ca) ratio is digested under high pressure and temperature (*P–T*) conditions (Takei *et al.* 2001). Unlike MgF_2, $CaAlF_5$ and ralstonite that commonly form during the digestion of basaltic samples with HF, AlF_3 is very stable and cannot be decomposed through heating with $HClO_4$. The formation of AlF_3 leads to an erroneous result owing to the incomplete recovery of IFFEs that coprecipitate with AlF_3. To summarise, the compositions of Ca, Al and Mg in the sample solution that ensures $> 95\%$ recovery yields for IFFEs and HFSEs are limited as presented by the crosshatched areas in Figure S1. These previous studies noted out that if the Ca-Al-Mg compositions in rock samples are inappropriate for measurements of IFFEs or HFSEs, the Ca-Al-Mg compositions should be adjusted by the addition of Mg or Al solutions.

In the present study, we specifically focus on the analysis of twenty-seven elements (Ti, Rb, Sr, Y, Zr, Nb, Cs, Ba, lanthanoids, Hf, Ta, Pb, Th and U) in rock samples by solution-based ICP-MS. These elements are the most frequently measured in modern geochemical applications. Of these elements, the twenty-two elements other than HFSEs (i.e., Rb, Sr, Y, Cs, Ba, lanthanoids, Pb, Th and U) are defined as IFFEs hereafter, because Yokoyama *et al.* (1999) confirmed the coprecipitation of them with insoluble fluorides. Considering the problems presented above regarding the individual chemical characteristics of IFFEs and HFSEs and the Ca-Al-Mg compositions in rock samples, we have developed a simultaneous method that determines the mass fractions of IFFEs and HFSEs using a solution prepared by the dissolution of a single aliquot of a rock sample, which aims to analyse (i) precious samples where the amounts available for analysis are limited and (ii) heterogeneous samples where the dissolution of two aliquots may give different results for some elements. In this study, mass fractions of Zr, Hf and Ti were determined by the isotope dilution (ID) method, whereas those of the other HFSEs and IFFEs were determined by the isotope dilution-internal standardisation (ID-IS) method using Zr-Hf and In-Tl internal standards. The precision and accuracy of the developed method were evaluated by analysing some rock geological reference materials.

Experiments

Instrumentation

Throughout this study, we used a quadrupole-type inductively coupled plasma-mass spectrometry (ICP-QMS) (X-Series 2; Thermo Fisher Scientific, Waltham, Massachusetts, USA) equipped with an autosampler (ASX-112FR; Teledyne CETAC Technologies, Omaha, Nebraska,

USA) installed at the Tokyo Institute of Technology (Tokyo Tech), Japan. The instrumental setting and the typical detection limits for these analytical elements of ICP-MS are described in Tables 1 and S1, respectively. We monitored the following isotopes: ^{85}Rb, ^{86}Sr, ^{89}Y, ^{133}Cs, ^{135}Ba, ^{139}La, ^{140}Ce, ^{141}Pr, ^{146}Nd, ^{147}Sm, ^{151}Eu, ^{157}Gd, ^{159}Tb, ^{163}Dy, ^{165}Ho, ^{166}Er, ^{169}Tm, ^{172}Yb, ^{175}Lu, ^{208}Pb, ^{232}Th and ^{238}U for the determination of the mass fractions of IFFEs, and $^{47, 49}$Ti, $^{90, 91}$Zr, ^{93}Nb, $^{178, 179}$Hf and ^{181}Ta for the determination of the mass fractions of HFSEs. In addition, ^{113}In, ^{115}In, ^{203}Tl, and ^{205}Tl were monitored for internal standardisation.

We used a high-pressure digestion system known as DAB-2 (maximum: 200 bar and 250 °C, Berghof, Germany) installed at Tokyo Tech for complete sample digestion. Samples were placed in a PTFE insert with acids, spike solutions and/or a standard solution of Al or Mg, and were installed in a stainless jacket, which was made from the alloy of SUS316Ti.

Reagents

High-purity de-ionised water (HPW: 18.2 MΩ cm) was prepared using a water purification system (Milli-Q Integral 5; Merck Millipore, Germany). HF (atomic absorption spectrometry (AAS) grade 30 mol l^{-1}, Kanto Chemical, Chuo-ku, Tokyo, Japan), HNO_3 (electronics industry (EL) grade 16 mol l^{-1}, Mitsubishi Chemical, Chiyoda-ku, Tokyo, Japan), HCl (EL grade 12 mol l^{-1}, Mitsubishi Chemical, Japan) and $HClO_4$ (TAMAPURE-AA-100 grade 12 mol l^{-1}, Tama Chemicals, Kawasaki, Kanagawa, Japan) were used for rock sample decomposition without purification by distillation. HF was distilled once by a two-bottle PTFE distillation system (1D HF) to make ^{91}Zr-, ^{179}Hf- and ^{49}Ti-enriched spikes. For making ^{113}In- and ^{203}Tl-enriched spikes, 1D HNO_3 was prepared by distilling HNO_3 (EL grade 16 mol l^{-1}) once in the same procedure as 1D HF.

Table 1.
Instrumental conditions for ICP-MS

Instrument	Quadrupole-type ICP-MS X-Series 2 (Thermo Scientific)
Autosampler	ASX-112FR (Teledyne CETAC Technologies)
Plasma power	1400 W
Plasma Ar gas flow rate	15–16 l min^{-1}
Auxiliary Ar gas flow rate	0.8–1.0 l min^{-1}
Nebuliser Ar gas flow rate	0.9–1.0 l min^{-1}
Cooling Ar gas flow rate	14–15 l min^{-1}
Skimmer cone	Ni, Xt for IFFEs; Pt Xs for HFSEs
Sampling cone	Ni/Cu for IFFEs; Pt for HFSEs
Torch	Quartz, O-ring free
Injector	Quartz in PFA base, 2.0 mm for IFFEs; Sapphire in PFA base, 2.0 mm for HFSEs
Nebuliser	PFA-ST MicroFlow Nebuliser (Elemental Scientific)
Spray chamber	Cyclonic, quartz, O-ring free (Elemental Scientific)
Spray chamber cooler	PC^3 Peltier cooler, +2 °C (Elemental Scientific)
Sample uptake rate	1000 µl min^{-1}
Typical oxide formation rate	CeO^+/Ce^+ = 0.02
Data acquisition (IFFEs)	10 ms/peak, 3 channels/mass, 32 scans/cycles, 5 cycles/run
Data acquisition (HFSEs)	10 ms/peak, 3 channels/mass, 32 scans/cycles, 10 cycles/run

HFSEs, high field-strength elements; ICP-MS, inductively coupled plasma-mass spectrometry; IFFEs, insoluble fluoride-forming elements.

An Al solution (10000 µg ml^{-1}, Agilent Technologies, Santa Clara, California, USA) and an Mg solution (AAS grade 1000 µg ml^{-1}, Kanto Chemical, Japan) were used for the adjustment of the Ca-Al-Mg compositions in the rock samples. Barium, Ce, Pr, Nd, Gd and Tb standard solutions (AAS grade, Kanto Chemical, Japan) were diluted and used for oxide and hydroxide corrections in the measurements of lanthanoids.

To determine the mass fractions of Nb and Ta by the ID-IS method, we used a custom-made mix standard solution (Cat. No. XSTC-3493-100, SPEX CertiPrep, Metuchen, New Jersey, USA) containing HFSEs in 1.7% HF (Ti: 4964 ± 30 µg g^{-1}, Zr: 98.8 ± 0.5 µg g^{-1}, Nb: 9.86 ± 0.05 µg g^{-1}, Hf: 2.96 ± 0.06 µg g^{-1} and Ta: 1.00 ± 0.02 µg g^{-1}). On the other hand, to determine the mass fractions of IFFEs by the ID-IS method, we used two standard solutions, XSTC-1 solution (SPEX CertiPrep, USA) containing Sc, Y, La, Ce, Pr, Nd, Sm, Eu, Gd, Tb, Dy, Ho, Er, Tm, Yb and Lu and HPS-1418-223-100 solution (High-Purity Standards, USA) containing Rb, Sr, Cs, Ba, Pb, Th and U in 0.5% HNO_3. The mass fraction of each element in the XSTC-1 solution is 10 µg g^{-1} and is certified with ± 0.5% uncertainty. In the HPS-1418-223-100 solution, the mass fractions of Ba and Sr are 100 ± 1 µg g^{-1}, that of Cs is 10.0 ± 0.2 µg g^{-1}, and those of the others are 10.0 ± 0.1 µg g^{-1}.

Three solutions with natural isotope compositions were prepared for the correction of mass fractionation during the ICP-MS measurements by ID method: A Ti (70 ng g^{-1}) solution in HF (0.5 mol l^{-1}) was made from the custom-made mix standard solution of HFSEs as noted above, a Zr (20 ng g^{-1}) and Hf (10 ng g^{-1}) mix solution in HF (0.5 mol l^{-1}) was prepared from Zr and Hf solutions (AAS grade 1000 µg ml^{-1}, Kanto Chemical, Japan), and an In (5 ng g^{-1}) and Tl (5 ng g^{-1}) mix solution in HNO_3 (0.5 mol l^{-1}) was prepared from In (AAS grade 1000 µg ml^{-1}, Elemental Standards, Everton Park, Queensland, Australia) and Tl solutions (AAS grade 1000 µg ml^{-1}, Wako, Japan). Enriched

isotopes of ^{49}Ti, ^{91}Zr, ^{179}Hf, ^{113}In and ^{203}Tl obtained from the Oak Ridge National Laboratory (Oak Ridge, Tennessee, USA) were used in this study. The ^{49}Ti, ^{91}Zr and ^{179}Hf spikes were used to determine Ti, Zr and Hf abundances in rock samples by the ID method and Nb and Ta abundances by the ID-IS method, whereas ^{113}In and ^{203}Tl spikes were prepared to obtain the mass fractions of IFFEs by the ID-IS method. The isotope enrichment and chemical formula of these enriched spikes were as follows: ^{49}Ti = 96.25% (TiO_2), ^{91}Zr = 94.59% (ZrO_2), ^{179}Hf = 86.87% (HfO_2), ^{113}In = 89.76% (In_2O_3) and ^{203}Tl = 97.10% (Tl_2O_3). These isotopic compositions in the spike solutions were certified by the Oak Ridge National Laboratory. The ^{49}Ti-enriched spike was dissolved using HF (1D) and HCl (EL grade) conditioned in HF (1D 3 mol l^{-1}, Ti = 85 μg g^{-1}). The ^{91}Zr- and ^{179}Hf-enriched spikes were individually dissolved using HF (1D) and conditioned in HF (0.5 mol l^{-1}). The ^{113}In- and ^{203}Tl-enriched spikes were prepared as described in Yokoyama *et al.* (2017). Subsequently, the ^{91}Zr-^{179}Hf-mixed and ^{113}In-^{203}Tl-mixed spike solutions were prepared separately by mixing individual spike solutions (Zr = 14 μg g^{-1}, Hf = 0.39 μg g^{-1}, In = 1.50 μg g^{-1} and Tl = 1.05 μg g^{-1}).

Geological reference materials

We analysed seven geological reference materials: JB-1a, JB-3, JR-2, JA-1, JA-2, JA-3 and JG-2, supplied by the Geological Survey of Japan (GSJ), and BHVO-2 supplied by the United States Geological Survey. JB-1a is a basalt from Kitamatsuura. JB-3 is a high-Al basalt from the Fuji volcano. JR-2 is a rhyolite from Wada Toge. JA-1, JA-2 and JA-3 are andesites from the Hakone volcano, Goshikidai sanukitoid and the Asama volcano, respectively. JG-2 is Naegi granite. BHVO-2 is a basalt from a Hawaiian volcano.

To prepare samples with specific major element compositions, the Al or Mg solutions were added to BHVO-2, JR-2 and JG-2. We synthesised seven types of samples with the following compositions: Ca:Al:Mg = 24:55:21 was prepared by adding the Al solution to BHVO-2 (referred to as BHVO-2+Al), Ca:Al:Mg = 13:75:12 was prepared by adding an excessive amount of the Al solution to BHVO-2 (referred to as BHVO-2+exAl), Ca:Al:Mg = 2.8:65:32 was prepared by adding the Mg solution to JR-2 (referred to as JR-2+Mg), Ca:Al:Mg = 1.7:38:60 was prepared by adding an excessive amount of the Mg solution to JR-2 (referred to as JR-2+exMg), Ca:Al:Mg = 3.4:60:37 was prepared by adding the Mg solution to JG-2 (referred to as JG-2+Mg), and Ca:Al:Mg = 2.9:51:46 was prepared by adding an excessive amount of the Mg solution to JG-2 (referred to as JG-2+exMg). The resulting Ca-Al-Mg compositions in individual sample solutions are shown in Figure S1 and Table S2.

Decomposition of rock samples

Separate method (Method A): Mass fractions of elements determined by the internal standardisation method are affected by differences in the standard material for calibration. To evaluate the simultaneous method developed in this study, we separately decomposed the geological reference materials and measured the mass fractions of IFFEs and HFSEs by following the conventional methods of Yokoyama *et al.* (2017) and Makishima and Nakamura (2000), respectively (separate method). This method is described as Method A hereafter. We can also exclude the effect of differences in the experimental conditions (e.g., instrument, decomposition condition of samples) and lot number of geological reference materials, by comparing the mass fractions of elements obtained by Method A and the simultaneous method.

Figure 1 shows the overview of the experimental procedure in this study. The mass fractions of IFFEs and HFSEs in JB-1a, JB-3, JR-2, JA-1, JA-2, JA-3, BHVO-2 and JG-2 were determined by Method A, respectively. It should be noted that BHVO-2+Al was used for the determination of the mass fractions of HFSEs in BHVO-2 because the Ca-Al-Mg composition of BHVO-2 is plotted in the region of the Ca-Al-Mg ternary plot where HFSEs coprecipitate with insoluble fluoride (Figure S1). Meanwhile, JG-2+exMg was prepared to determine the mass fractions of IFFEs in JG-2 as insoluble AlF_3, which incorporates some of the IFFEs, is formed during the digestion of rock samples with a high Al/(Mg+Ca) ratio using DAB-2, which can digest the refractory minerals (e.g., zircon) in JG-2.

For the determination of the mass fractions of IFFEs in all analytical samples except for JG-2, a powdered rock sample (approximately 50 mg) was weighed into a perfluoroalkoxy alkane (PFA) vessel (7 ml) together with ^{113}In-^{203}Tl-mixed spike. After the addition of HF (1 ml, 30 mol l^{-1}, AAS grade), HNO_3 (1 ml, 16 mol l^{-1}, EL grade) and $HClO_4$ (1 ml 12 mol l^{-1}), the vessel was tightly capped and agitated in an ultrasonic bath for 30 min. The vessel was heated in a stepwise fashion (120 °C for 12 h, 165 °C for 16 h and 195 °C until the sample was dry). This procedure was repeated twice to suppress the formation of insoluble fluorides. After treatment with HCl (6 mol l^{-1}), the sample was diluted with HNO_3 (0.5 mol l^{-1}) to measure the IFFEs with ICP-MS by the ID-IS method. For JG-2 (JG-2+exMg), a rock powder (approx. 200 mg) was weighed in a PTFE insert (50 ml) of DAB-2 together with the

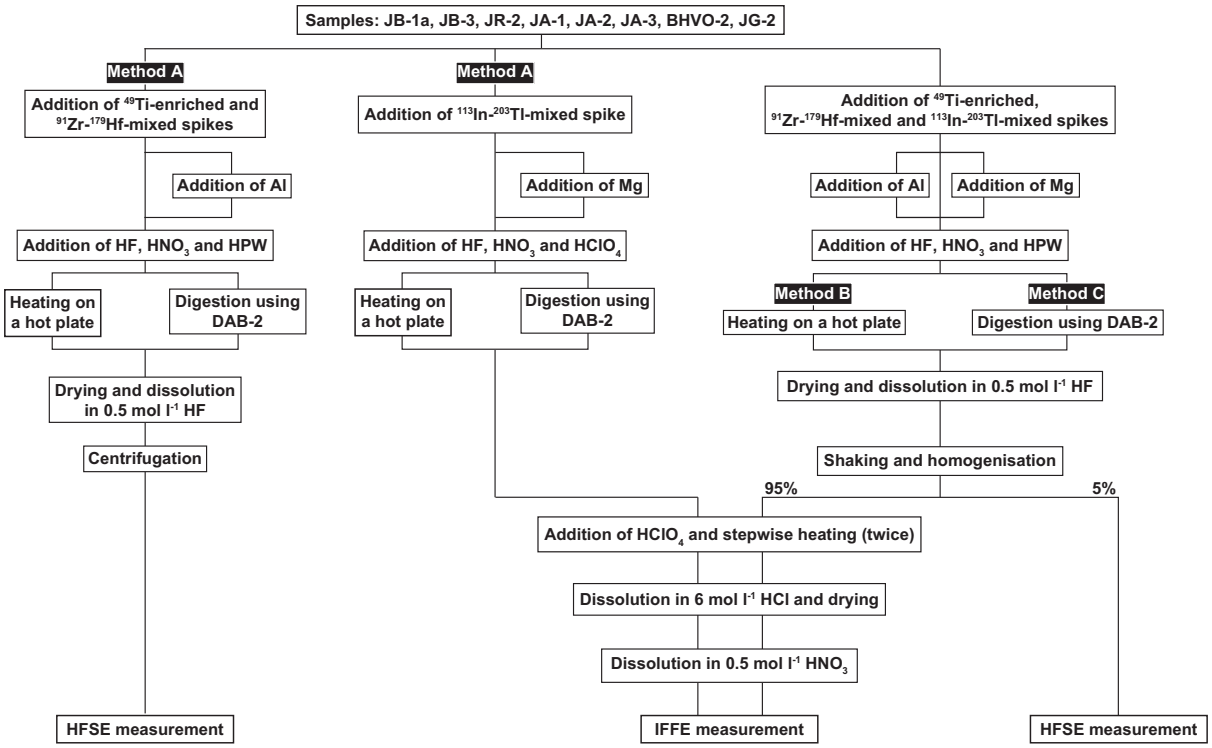

Figure 1. Overview of experimental procedures conducted in this study.

^{113}In-^{203}Tl-mixed spike, the Mg solution, HF (30 mol l^{-1}), HNO_3 (16 mol l^{-1}) and HPW. We prepared a relatively large amount of JG-2 compared with that of the other geological reference materials to minimise the heterogeneity of the trace element-rich accessory minerals such as zircon (i.e., the nugget effect). The sample in the insert was dissolved in the digestion system at 225 °C for 48 h to ensure complete dissolution of refractory minerals. Then, the solution was transferred to a clean PFA vessel (7 ml) and $HClO_4$ (1 ml 12 mol l^{-1}) was added. The vessel was heated on a hot plate in a stepwise fashion. The subsequent procedure was the same as described for Method A in the IFFE measurements of the other samples.

For the determination of mass fractions of HFSEs in all analytical samples except for JG-2, the powdered rock sample (approximately 50 mg) was weighed into a PFA vessel (7 ml) together with ^{49}Ti-enriched spike and the ^{91}Zr-^{179}Hf-mixed spike. After the addition of HF (1 ml, 30 mol l^{-1}, AAS grade), HNO_3 (1 ml, 16 mol l^{-1}, EL grade) and HPW (1 ml), the vessel was tightly capped and agitated in an ultrasonic bath for 30 minutes. It should be noted that an Al solution was also added to BHVO-2 (BHVO-2+Al) before sample digestion. The vessel was heated at 120 °C on a hot plate overnight for sample digestion and for obtaining a spike-sample isotopic equilibrium. Then, the cap was opened, and the sample was dried at 120 °C on a hot plate. The dried sample was dissolved in HF (5 ml, 0.5 mol l^{-1}) and centrifuged. The supernatant solution was diluted with HF (0.5 mol l^{-1}) and used for the measurement of HFSEs using ICP-MS by the ID method for Ti, Zr and Hf and the ID-IS method for Nb and Ta. For JG-2, approximately 200 mg was weighed in a PTFE insert (50 ml) of DAB-2 together with the same acids and spikes as described for Method A in the HFSE measurements of the other samples. The sample in the insert was dissolved in the digestion system at 225 °C for 48 h to ensure complete dissolution of refractory minerals. Then, the solution was transferred to a clean PFA vessel (7 ml) and dried at 120 °C on a hot plate. The subsequent procedure is the same as Method A for the determination of HFSEs in other samples described above.

Simultaneous method with hot plate digestion (Method B): The mass fractions of IFFEs and HFSEs in JB-1a, JB-3, JR-2, JR-2+exMg, JA-2, BHVO-2 and BHVO-2+Al were determined by the simultaneous method after sample digestion with acids on a hot plate. This procedure is called 'Method B' hereafter to distinguish the simultaneous method in which the rock samples were digested with DAB-2 (Method C; see the next section). We note that the mass fractions of IFFEs and HFSEs in JG-2 were not determined by Method B because JG-2 includes refractory minerals such as zircon, which cannot be digested with acids on a hot plate.

A powdered rock sample (approximately 50 mg) was weighed into a PFA vessel (7 ml) together with the ^{49}Ti-enriched spike, the ^{91}Zr-^{179}Hf-mixed spike and the ^{113}In-^{203}Tl-mixed spike. After the addition of HF (1 ml, 30 mol l^{-1}, AAS grade), HNO_3 (1 ml, 16 mol l^{-1}, EL grade) and HPW (1 ml), the vessel was tightly capped and agitated in an ultrasonic bath for 30 min. The vessel was heated at 120 °C on a hot plate overnight, and then, the sample was dried on a hot plate at 120 °C. The dried sample was dissolved in HF (5 ml, 0.5 mol l^{-1}). The sample solution containing insoluble fluorides was thoroughly shaken and homogenised by agitating in an ultrasonic bath until the solution became a milky suspended solution without visible precipitates (approximately 6 h). Immediately after the homogenisation, an aliquot (approximately 5%) of the suspended solution was transferred to a polypropylene tube (2 ml) and centrifuged. The supernatant was diluted with HF (0.5 mol l^{-1}) and used for the measurement of HFSEs by ICP-MS through the ID method for Ti, Zr and Hf and by the ID-IS method for Nb and Ta.

For the determination of IFFEs, $HClO_4$ (1 ml, 12 mol l^{-1}) was added into the remaining (approx. 95%) of the suspended sample solution in the PFA vessel. The vessel was heated in a stepwise fashion (120 °C for 12 h, 165 °C for 16 h and 195 °C until the sample was dry). This procedure was repeated twice to suppress the formation of insoluble fluorides. After the treatment with HCl (6 mol l^{-1}), the sample was diluted with HNO_3 (0.5 mol l^{-1}) to measure IFFEs with ICP-MS.

Simultaneous method with DAB-2 digestion (Method C): Method B described above cannot be applied to samples containing acid-resistant, refractory minerals such as zircon and spinel. These samples need to be digested under high *P–T* conditions using DAB-2. Therefore, we conducted the simultaneous method coupled with a high *P–T* sample digestion using the high-pressure digestion system, DAB-2. The performance of this procedure, which is named Method C, was evaluated by determining the mass fractions of IFFEs and HFSEs in JB-1a, JB-3, JR-2+Mg, JR-2+exMg, JA-1, JA-2, JA-3, BHVO-2, BHVO-2+Al, BHVO-2+exAl, JG-2+Mg and JG-2+exMg.

The powdered sample (approx. 50 mg) was weighed into a PTFE insert (50 ml) of DAB-2 together with ^{49}Ti-enriched spike, ^{91}Zr-^{179}Hf-mixed spike, ^{113}In-^{203}Tl-mixed spike, HF (30 mol l^{-1}), HNO_3 (16 mol l^{-1}) and HPW. The amounts of acids and spikes were the same as those in Method B. The sample in the insert was dissolved in the digestion system at 225 °C for 48 h to ensure complete dissolution of refractory minerals. Then, the solution was transferred to a clean PFA vessel (7 ml), dried on a hot plate and dissolved in HF (5 ml, 0.5 mol l^{-1}). The subsequent procedure for HFSE and IFFE measurements followed the steps as Method B.

Determination of elemental abundances in rock samples

In this study, the ID and ID-IS methods were used to determine the mass fractions of Zr, Hf and Ti and the other elements, respectively. The principles of the ID and ID-IS methods are described in detail in the Appendix S1. The sensitivity variation during ICP-MS analysis is mass-dependent and correlates linearly with the ratio of mass and electrical charge (*m/z*, Yokoyama *et al.* 2017). The internal standard elements for the determination of Nb and Ta by the ID-IS method were ^{91}Zr and ^{179}Hf, respectively, which corrects for sensitivity variation. For the IFFE measurements, the sensitivity variation was corrected by the internal standard elements ^{113}In and ^{203}Tl.

The formation of oxides and hydroxides for Ba and REEs interferes with heavier REEs than Sm (e.g., ^{143}Nd^{16}O on ^{159}Tb). To determine the precise mass fraction of IFFEs, the correction of the oxide and hydroxide formation is important. The correction method is also shown in detail in the online Appendix S1.

For the determination of Nb, Ta and IFFEs by the ID-IS method, we used multi-element standard solutions in this study, which are frequently used in measurement calibration of geological reference materials. For instance, the variation for previously reported IFFE mass fractions for the geological reference material JB-3 is approximately 10% (2*s*, n = 6–8), whereas the mass fractions of HFSEs excluding Ti is > 10% (2*s*, n = 4–7) (Imai *et al.* 1995, Makishima *et al.* 1999, Makishima *et al.* 2000, Dulski 2001, Orihashi and Hirata 2003, Awaji *et al.* 2006, Makishima and Nakamura 2006, Lu *et al.* 2007, Kon and Hirata 2015, Kamei 2016, Yokoyama *et al.* 2017) (Table S3). Therefore, to determine the precise and correct mass fractions, it is important to use certified standard solutions.

Results

Chemical blanks

All blank runs were performed under the same conditions of rock sample digestion (50 mg of the sample). The total chemical blanks of IFFEs and HFSEs in the procedures (Method A, Method B and Method C) are shown in Table 2. The results indicate that the blank contribution in all methods was < 0.1%

for most elements in all samples except for Ta (< 0.9%) and Cs (< 0.3%; Method C). In most cases, the total chemical blanks of IFFEs through Method C are higher than those for Method B (Table 2). The total digestion time of Method C is longer than Method B, which could be the main reason for the increase in the chemical blanks for Method C. On the other hand, the total chemical blanks of HFSEs in Method C are mostly similar to those in Method B. This result suggested that the long total digestion time did not affect the total blanks of HFSEs. In addition, we performed the cleaning of PTFE insert of the digestion system DAB-2 before sample digestion using DAB-2. The details are described below in the section 'Reduction in chemical blanks through Method C' of the Discussion. In this study, the blank correction was conducted by subtracting the total chemical blanks in Table 2.

Verification of Method A

Table 3 shows the mass fractions of twenty-seven elements in JB-1a, JB-3, JR-2, JA-1, JA-2, JA-3, BHVO-2 and JG-2 determined by Method A. The mass fractions of HFSEs in an Al-poor sample BHVO-2 and IFFEs in an Al-rich sample JG-2 were determined by measuring those in BHVO-2+Al and JG-2+exMg to avoid the possible loss of HFSEs and IFFEs owing to the coprecipitation with insoluble fluorides, respectively (Figure S1a). The precision of each element (1*s*) for all replicate analyses of each sample was generally < 3%. In Table 3, the mass fractions of individual elements in these samples obtained by Method A are compared with those reported by the previous studies: Jochum *et al.* (2015), Imai *et al.* (1995), Kon and Hirata (2015) and/or Kamei (2016). The mass fraction data in Jochum *et al.* (2015) and Imai *et al.* (1995) are a compilation of literature data. In contrast, those in Kon and Hirata (2015) and Kamei (2016) were obtained by measuring the element abundances in glass beads of rock samples prepared by fusion with $Li_2B_4O_7$: The procedure is considered to completely digest refractory minerals in rock samples without HF. Kon and Hirata (2015) measured the beads with ICP-MS coupled with the femtosecond laser ablation, whereas Kamei (2016) decomposed the bead with some acids and analysed the samples with solution-based ICP-MS.

Table 2.
Total chemical blanks in each sample digestion procedure

	Method A	Method B	Method C
(ng)			
Ti	9.8	12	26
(pg)			
Zr	209	258	377
Nb	< 66	< 65	24
Hf	82	63	62
Ta	34	40	42
Rb	*6.9*	< 1.5	19
Sr	*50*	< 33	161
Y	*2.0*	4.5	4.7
Cs	*6.6*	1.0	15
Ba	*48*	50	266
La	*1.5*	1.8	5.9
Ce	*2.9*	4.8	9.4
Pr	*0.34*	0.75	20
Nd	*1.3*	< 4.4	164
Sm	*0.42*	< 0.81	1.1
Eu	*0.069*	0.28	0.74
Gd	*0.36*	1.6	2.1
Tb	*0.091*	0.11	0.58
Dy	*0.23*	0.54	1.0
Ho	*0.055*	< 0.083	0.76
Er	*0.31*	0.63	1.6
Tm	*0.041*	0.10	1.0
Yb	*0.51*	40	41
Lu	*0.071*	0.32	1.4
Pb	*12*	33	105
Th	*0.48*	1.4	3.1
U	*1.1*	1.7	14

These data are averaged for each elements in Method A (n = 2), B and C (n = 4). Italics represent the data obtained from Yokoyama *et al.* (2017).

As shown in Table 3, the mass fractions of all determined elements in the samples obtained through Method A are in good agreement with those from one or more literature data at ± 5%. Some of the inconsistencies in the mass fractions, of which the difference between this study and the literature data is approximately ± 10%, could be attributed to the difference in the used reference materials and their working values or resulted from an inappropriate analytical protocol conducted in previous studies. The latter would be the case for the mismatch in the mass fraction of Ti in JR-2, of which the difference between this study and Imai *et al.* (1995) reached -17%. The sample heterogeneity associated with the presence of Ti-rich accessory minerals (i.e., the nugget effect) is unlikely because JR-2 is a glassy obsidian and the repeatability of Ti abundance obtained by Method A was 0.81% (1*s*). Rather, the inconsistency is owing to the relatively low mass fraction of Ti in JR-2 such that precise determination with a conventional X-ray fluorescence (XRF) method and neutron-capture prompt-gamma activation analysis (PGAA) was difficult. In fact, the mass fraction of Ti in JR-2 reported in six previous studies varied largely from 300 μg g^{-1} to 485 μg g^{-1} (GeoReM, Stix *et al.* 1996, Iida *et al.* 2003, Gméling *et al.* 2005, Nakayama and Nakamura 2005, Sano *et al.* 2006, Riley *et al.* 2016). Likewise, the mass fraction of Eu in JG-2 is also relatively low, which caused the large difference between this study and previous studies. This mass fraction of Eu in JG-2 is within the range of the reported values previously. On the other hand, the

Table 3.
Mass fractions of IFFEs and HFSEs in rock samples decomposed by Method A, the repeatability of each analysis and relative difference to references (with the references)

Sample	JB-1a						JB-3									
Composition	JB-1a						JB-3									
			Jochum *et al.* (2015)		Kon and Hirata (2015)				Yokoyama *et al.* (2017)		Imai *et al.* (1995)		Kon and Hirata (2015)		Kamei (2016)	
(μg g^{-1})	*n* = 3	% RSD	Value	Diff. %	Value	Diff. %	*n* = 3	% RSD	Value	Diff. %	Value	Diff. %	Value	Diff. %	Value	Diff. %
Ti	7575	0.8	7731	-2.0	7588	-0.2	8463	0.9			8630	-1.9	8487	-0.3	n.d.	-
Zr	135	0.6	140	-3.8	134	0.8	91.0	0.3			97.8	-6.9	91.8	-0.9	94.2	-3.4
Nb	27.2	0.6	27.6	-1.3	27.8	-2.2	1.95	2.9			2.47	-21	2.07	-5.8	1.96	-0.5
Hf	3.52	0.6	3.47	1.5	3.36	4.8	2.71	0.5			2.67	1.5	2.61	3.8	2.84	-4.6
Ta	1.68	0.3	1.74	-3.5	1.67	0.7	0.130	2.8			0.15	-13	0.126	2.9	0.331	-61
Rb	36.5	0.3	38.2	-4.2	37.3	-2.0	14.0	0.3	13.8	1.5	15.1	-7.3	14.2	-1.1	14.2	-1.4
Sr	442	0.3	443	-0.3	443	-0.2	412	0.3	408	1.0	403	2.2	411	0.2	401	2.7
Y	20.4	1.2	22.9	-11.2	22.4	-9.0	23.6	0.4	23.3	1.2	26.9	-12.2	25.6	-7.7	25.9	-8.8
Cs	1.23	0.5	1.22	1.5	1.22	0.8	0.951	0.3	0.917	3.7	0.94	1.2	0.936	1.6	0.917	3.7
Ba	504	0.9	495	1.9	494	2.1	245	0.3	238	3.0	245	0.0	237	3.3	242	1.2
La	37.7	0.8	37.7	-0.1	37.1	1.7	8.55	0.5	8.08	5.8	8.81	-2.9	8.37	2.2	8.45	1.2
Ce	66.2	0.6	65.9	0.4	65.0	1.8	21.8	0.6	20.5	6.0	21.5	1.3	21.1	3.2	21.0	3.7
Pr	7.04	0.7	7.10	-0.9	6.92	1.7	3.30	0.2	3.15	4.8	3.11	6.1	3.19	3.5	3.24	1.9
Nd	26.3	0.6	26.2	0.6	25.8	1.9	16.1	0.6	15.6	3.3	15.6	3.5	15.6	3.3	15.7	2.8
Sm	5.08	0.9	5.10	-0.4	5.01	1.3	4.35	0.6	4.25	2.5	4.27	2.0	4.21	3.4	4.35	0.1
Eu	1.46	0.9	1.48	-1.6	1.46	0.1	1.33	0.6	1.30	1.7	1.32	0.4	1.29	3.2	1.37	-3.2
Gd	5.08	1.3	4.70	8.0	4.62	9.9	4.86	0.7	4.72	3.0	4.67	4.1	4.53	7.3	4.70	3.4
Tb	0.712	1.6	0.699	1.8	0.694	2.5	0.762	0.4	0.737	3.4	0.73	4.4	0.727	4.8	0.776	-1.8
Dy	4.16	1.3	4.07	2.1	4.00	3.9	4.72	0.7	4.64	1.8	4.54	3.9	4.45	6.0	4.61	2.3
Ho	0.807	1.4	0.805	0.3	0.774	4.3	0.965	0.7	0.949	1.6	0.80	20.6	0.907	6.4	0.961	0.4
Er	2.27	1.7	2.23	1.6	2.18	4.0	2.77	0.6	2.76	0.5	2.49	11.4	2.58	7.5	2.69	3.1
Tm	0.321	1.6	0.320	0.5	0.319	0.8	0.397	0.9	0.394	0.8	0.42	-5.4	0.387	2.7	0.437	-9.1
Yb	2.06	1.2	2.10	-2.1	1.97	4.4	2.58	0.8	2.57	0.1	2.55	1.1	2.45	5.2	2.42	6.5
Lu	0.302	2.0	0.315	-4.0	0.291	3.8	0.359	0.5	0.385	-6.9	0.39	-8.0	0.365	-1.7	0.390	-8.0
Pb	6.10	0.2	6.44	-5.4	6.24	-2.3	4.79	0.7	5.01	-4.5	5.58	-14.2	4.93	-2.9	4.93	-2.9
Th	8.99	0.6	8.97	0.2	8.85	1.6	1.29	2.6	1.30	-1.2	1.27	1.3	1.26	2.2	1.25	2.9
U	1.65	0.3	1.62	2.1	1.62	2.0	0.487	1.8	0.479	1.6	0.48	1.4	0.473	2.9	0.496	-1.9

Sample	JR-2								JA-1							
Composition	JR-2								JA-1							
			Imai *et al.* (1995)		Kon and Hirata (2015)		Kamei (2016)				Jochum *et al.* (2015)		Kon and Hirata (2015)		Kamei (2016)	
(μg g^{-1})	*n* = 3	% RSD	Value	Diff. %	Value	Diff. %	Value	Diff. %	*n* = 3	% RSD	Value	Diff. %	Value	Diff. %	Value	Diff. %
Ti	350	0.8	420	-17	n.d.	-	n.d.	-	4962	0.3	5094	-2.0	5004	-0.3	-	-
Zr	85.7	0.3	96.3	-11	93.0	-7.8	96.2	-11	79.6	0.3	83.7	-3.5	80.3	0.6	84.4	-4.3
Nb	17.6	3.0	18.7	-5.8	18.9	-6.7	17.7	-0.5	1.20	3.6	1.33	-8.9	1.32	-8.2	1.23	-1.2
Hf	5.17	0.4	5.14	0.5	5.32	-2.8	5.42	-4.6	2.49	0.9	2.51	0.3	2.39	5.3	2.69	-6.5
Ta	2.10	2.6	2.29	-8.5	2.17	-3.3	2.17	-3.4	0.0939	1.6	0.0979	-2.4	0.0920	3.9	0.157	-39

Table 3 (continued).

Sample	JR-2								JA-1							
Composition	JR-2		Imai *et al.* (1995)		Kon and Hirata (2015)		Kamei (2016)		JA-1		Jochum *et al.* (2015)		Kon and Hirata (2015)		Kamei (2016)	
(μg g^{-1})	*n* = 3	% RSD	Value	Diff. %	Value	Diff. %	Value	Diff. %	*n* = 3	% RSD	Value	Diff. %	Value	Diff. %	Value	Diff. %
Rb	301	0.8	303	-0.6	303	-0.6	296	1.8	10.7	0.1	11.0	-3.2	10.8	-1.2	10.7	-0.3
Sr	8.09	2.1	8.11	-0.3	n.d.	-	8.05	0.5	262	0.1	259	-2.0	257	-1.1	260	-2.2
Y	44.3	1.7	51.1	-13	48.7	-8.9	49.3	-10.1	26.4	0.3	28.0	-9.4	28.3	-10	28.7	-12
Cs	26.1	0.5	25.0	4.6	25.7	1.6	25.3	3.4	0.640	0.1	0.627	1.8	0.634	0.7	0.612	4.3
Ba	28.8	0.6	39.5	-27	28.3	1.7	29.6	-2.8	309	0.4	304	-2.0	298	0.0	308	-3.3
La	15.3	1.1	16.3	-6.1	14.9	3.1	15.3	0.0	5.06	0.4	4.88	-9.8	4.84	-9.1	4.97	-11
Ce	37.7	0.6	38.8	-2.9	36.8	2.3	37.6	0.2	13.5	0.2	13.2	-4.5	13.0	-3.0	13.1	-4.1
Pr	4.84	0.8	4.75	1.8	4.72	2.5	4.85	-0.3	2.15	0.7	2.08	-6.4	2.06	-5.4	2.13	-8.5
Nd	19.4	0.9	20.4	-5.1	19.0	1.6	19.3	0.3	11.1	0.5	10.7	-4.6	10.6	-4.1	10.6	-3.8
Sm	5.36	0.2	5.63	-4.8	5.26	1.9	5.38	-0.4	3.48	0.5	3.40	-5.8	3.30	-3.0	3.38	-5.3
Eu	0.0965	1.8	0.14	-31	n.d.	-	0.103	-6.3	1.10	0.4	1.11	-6.6	1.11	-6.0	1.16	-10
Gd	5.93	0.4	5.83	1.6	5.70	4.0	5.78	2.5	4.37	0.6	4.15	-1.4	4.14	-1.1	4.31	-5.0
Tb	1.03	0.8	1.10	-6.5	1.05	-1.9	1.01	1.9	0.755	0.1	0.727	-1.7	0.719	-0.6	0.731	-2.2
Dy	6.77	0.8	6.63	2.1	6.79	-0.3	6.65	1.8	4.93	0.2	4.75	-0.7	4.63	1.9	4.84	-2.6
Ho	1.45	0.7	1.39	4.1	1.46	-1.1	1.40	3.3	1.05	0.2	1.03	-2.7	0.998	0.6	1.03	-2.5
Er	4.62	0.8	4.36	5.9	4.60	0.4	4.66	-0.9	3.11	0.2	2.96	1.4	2.92	2.8	3.08	-2.6
Tm	0.751	0.5	0.74	1.5	0.779	-3.6	0.750	0.1	0.455	0.5	0.445	-0.8	0.447	-1.2	0.462	-4.4
Yb	5.35	0.3	5.33	0.4	5.40	-0.9	5.37	-0.4	3.02	0.4	2.95	-0.1	2.85	3.3	2.97	-0.9
Lu	0.817	0.3	0.88	-7.2	0.843	-3.1	0.807	1.2	0.440	0.4	0.454	-0.9	0.434	3.7	0.464	-3.0
Pb	21.2	0.6	21.5	-1.3	22.6	-6.2	21.3	-0.4	5.38	0.5	5.86	-4.2	5.48	2.5	5.49	2.3
Th	31.5	1.2	31.4	0.5	31.4	0.5	29.8	5.9	0.770	0.8	0.761	-3.4	0.728	0.9	0.699	5.1
U	11.1	1.2	10.9	1.6	11.2	-0.7	10.3	7.5	0.369	0.6	0.340	7.6	0.350	4.5	0.380	-3.7

Sample	JA-2										JA-3							
Composition	JA-2		Yokoyama *et al.* (2017)		Jochum *et al.* (2015)		Kon and Hirata (2015)		Kamei (2016)		JA-3		Kamei (2016)		Imai *et al.* (1995)		Kon and Hirata (2015)	
(μg g^{-1})	*n* = 3	% RSD	Value	Diff. %	Value	Diff. %	Value	Diff. %	Value	Diff. %	*n* = 3	% RSD	Value	Diff. %	Value	Diff. %	Value	Diff. %
Ti	3961	1.2			4013	-1.3	3974	-0.3	n.d.	-	4031	0.3	-	-	4195	-3.9	4063	-0.8
Zr	108	0.6			109	-0.8	108	-0.6	112	-3.9	110	0.3	115	-4.6	118	-7.0	111	-1.2
Nb	8.85	1.5			9.30	-4.8	9.09	-2.6	8.82	0.4	2.94	1.0	2.98	-1.4	3.41	-14	3.14	-6.4
Hf	2.85	0.4			2.84	0.4	2.77	2.9	3.04	-6.3	3.23	0.5	3.23	0.0	3.42	-5.6	3.11	3.8
Ta	0.645	0.9			0.652	-1.0	0.646	-0.1	0.766	-16	0.240	1.4	0.269	-11	0.27	-11	0.238	0.8
Rb	67.9	0.4	70.2	-3.3	69.8	-2.8	68.5	-0.9	65.9	3.0	35.2	0.4	34.0	3.6	36.7	-4.0	34.8	1.2
Sr	244	0.6	247	-1.2	246	-0.7	239	2.1	245	-0.4	290	0.4	280	3.4	287	0.9	280	3.4
Y	15.4	0.6	15.4	0.2	16.9	-8.7	16.8	-8.2	16.9	-8.7	18.1	0.2	19.6	-7.8	21.2	-15	19.5	-7.3
Cs	4.66	0.4	4.91	-5.1	4.78	-2.5	4.7	-0.8	4.46	4.5	2.15	0.2	2.16	-0.5	2.08	3.3	2.06	4.3

Table 3 (continued).

Sample	JA-2										JA-3							
Composition	JA-2										JA-3							
			Yokoyama *et al.* (2017)		Jochum *et al.* (2015)		Kon and Hirata (2015)		Kamei (2016)				Kamei (2016)		Imai *et al.* (1995)		Kon and Hirata (2015)	
(μg g^{-1})	*n* = 3	% RSD	Value	Diff. %	Value	Diff. %	Value	Diff. %	Value	Diff. %	*n* = 3	% RSD	Value	Diff. %	Value	Diff. %	Value	Diff. %
Ba	313	0.3	318	-1.5	308	1.6	302	3.7	316	-0.9	328	0.3	317	3.6	323	1.7	307	7.0
La	15.7	0.2	15.5	1.0	15.5	1.2	15.3	2.3	15.5	1.0	9.54	0.0	9.22	3.4	9.33	2.2	9.09	4.9
Ce	33.0	0.4	32.5	1.4	32.9	0.3	31.7	3.9	32.0	3.0	22.3	0.3	21.2	5.4	22.8	-2.0	21.1	5.9
Pr	3.69	0.4	3.69	-0.1	3.69	-0.1	3.52	4.7	3.71	-0.6	2.91	0.3	2.80	4.1	2.40	21	2.74	6.3
Nd	14.3	0.5	14.5	-1.2	14.0	2.0	13.7	4.6	14.1	1.6	12.7	0.3	12.1	5.2	12.3	3.5	12.0	6.1
Sm	3.09	0.5	3.10	-0.3	3.03	1.9	2.96	4.4	3.15	-1.9	3.17	0.2	3.05	3.8	3.05	3.8	2.97	6.6
Eu	0.870	0.5	0.892	-2.5	0.893	-2.6	0.853	2.0	0.956	-9.0	0.783	0.3	0.823	-4.9	0.82	-4.5	0.772	1.4
Gd	3.28	0.8	3.11	5.3	3.01	8.7	2.93	12	3.07	6.7	3.48	0.2	3.31	5.0	2.96	17	3.15	10
Tb	0.487	0.8	0.479	1.7	0.479	1.8	0.468	4.1	0.501	-2.8	0.546	0.2	0.535	2.0	0.52	4.9	0.519	5.1
Dy	2.99	0.4	2.98	0.4	2.85	4.9	2.83	5.7	2.89	3.5	3.42	0.2	3.28	4.2	3.01	14	3.17	7.8
Ho	0.611	0.2	0.607	0.6	0.591	3.3	0.577	5.9	0.612	-0.2	0.707	0.1	0.673	5.1	0.51	39	0.658	7.5
Er	1.77	0.7	1.78	-0.6	1.68	5.6	1.64	7.9	1.80	-1.7	2.09	0.1	2.04	2.4	1.57	33	1.95	7.1
Tm	0.257	0.9	0.259	-0.7	0.255	1.0	0.252	2.1	0.285	-9.7	0.308	0.5	0.303	1.7	0.28	10	0.299	3.1
Yb	1.69	0.8	1.71	-1.3	1.65	2.6	1.58	6.9	1.70	-0.7	2.04	0.5	2.01	1.7	2.16	-5.4	1.92	6.5
Lu	0.237	0.9	0.257	-7.8	0.255	-7.0	0.245	-3.2	0.273	-13	0.292	0.0	0.303	-3.5	0.32	-8.6	0.294	-0.5
Pb	18.0	0.3	19.6	-8.3	18.9	-4.8	19.4	-7.3	19.2	-6.4	7.50	0.2	7.58	-1.0	7.70	-2.5	7.53	-0.3
Th	4.86	0.2	5.02	-3.2	4.80	1.3	4.70	3.4	4.68	3.9	3.23	0.6	3.12	3.6	3.25	-0.6	3.13	3.2
U	2.28	0.2	2.28	0.1	2.18	4.6	2.19	4.2	2.14	6.7	0.999	0.6	0.923	8.2	1.18	-15	0.956	4.5

Sample	BHVO-2								JG-2									
Composition	BHVO-2		BHVO-2+Al						JG-2		JG-2+exMg							
					Jochum *et al.* (2015)		Kon and Hirata (2015)						Kon and Hirata (2015)		Kamei (2016)		Imai *et al.* (1995)	
(μg g^{-1})	*n* = 3	% RSD	*n* = 3	% RSD	Value	Diff. %	Value	Diff. %	*n* = 3	% RSD	*n* = 3	% RSD	Value	Diff. %	Value	Diff. %	Value	Diff. %
Ti			16562	1.5	16368	1.2	16506	0.3	269	1.9			n.d.	-	n.d.	-	264	1.9
Zr			168	0.9	171	-1.9	172	-2.2	111	3.0			105	5.4	112	-1.2	97.6	13
Nb			17.5	1.9	18.1	-3.1	18.6	-5.7	14.1	3.5			15.3	-7.5	15.2	-7.1	14.7	-4.0
Hf			4.48	1.5	4.47	0.1	4.40	1.8	5.30	3.3			4.99	6.3	5.24	1.2	4.73	12
Ta			1.14	1.8	1.15	-1.3	1.16	-2.0	1.74	3.2			2.30	-24	2.58	-33	2.76	-37
Rb	9.00	0.5			9.26	-2.9	9.09	-1.1			301	1.5	295	2.1	284	6.0	301	0.0
Sr	397	0.2			394	0.8	400	-0.6			16.7	1.7	n.d.	-	16.5	1.0	17.9	-6.9
Y	23.4	0.9			25.9	-9.7	26.3	-11			75.4	1.7	84.4	-11	86.3	-13	86.5	-13
Cs	0.101	3.3			0.0996	1.1	n.d.	-			7.22	1.1	6.98	3.4	7.14	1.1	6.79	6.3
Ba	132	0.6			131	1.1	132	0.5			65.5	1.6	56.8	15	66.8	-1.9	81.0	-19
La	15.3	0.3			15.2	0.9	15.4	-0.6			19.5	0.4	19.0	2.9	19.4	0.6	19.9	-2.0
Ce	37.8	0.2			37.5	0.8	37.6	0.7			47.7	1.1	46.9	1.6	47.3	0.8	48.3	-1.3
Pr	5.29	0.3			5.34	-0.9	5.29	0.0			6.16	0.7	5.98	3.1	6.16	0.1	6.20	-0.6

Table 3 (continued).

Sample	BHVO-2								JG-2									
Composition	BHVO-2		BHVO-2+Al						JG-2		JG-2+exMg							
					Jochum *et al.* (2015)		Kon and Hirata (2015)						Kon and Hirata (2015)		Kamei (2016)		Imai *et al.* (1995)	
(μg g^{-1})	*n* = 3	% RSD	*n* = 3	% RSD	Value	Diff. %	Value	Diff. %	*n* = 3	% RSD	*n* = 3	% RSD	Value	Diff. %	Value	Diff. %	Value	Diff. %
Nd	24.6	0.7			24.3	1.2	24.6	-0.4			25.3	0.8	24.7	2.3	25.5	-0.8	26.4	-4.2
Sm	6.10	0.5			6.02	1.4	6.09	0.3			7.93	0.9	7.76	2.1	8.18	-3.1	7.78	1.9
Eu	2.04	0.3			2.04	-0.2	2.07	-1.5			0.0853	0.4	n.d.	-	0.098	-13	0.10	-15
Gd	6.48	1.4			6.21	4.4	6.25	3.7			9.51	1.4	9.20	3.4	9.74	-2.4	8.01	19
Tb	0.935	1.0			0.939	-0.5	0.953	-1.9			1.76	3.0	1.78	-1.1	1.88	-6.2	1.62	8.9
Dy	5.27	1.1			5.28	-0.3	5.29	-0.5			11.6	1.8	11.9	-2.4	12.5	-6.7	10.5	11
Ho	0.969	0.6			0.989	-2.0	0.978	-0.9			2.47	2.2	2.59	-4.7	2.69	-8.2	1.67	48
Er	2.51	0.6			2.51	0.0	2.50	0.4			7.58	2.2	8.00	-5.3	8.49	-11	6.04	25
Tm	0.329	0.9			0.335	-1.9	0.343	-4.3			1.19	0.9	1.27	-6.8	1.30	-8.7	1.16	2.3
Yb	1.96	1.3			1.99	-1.6	2.01	-2.4			7.97	3.5	8.22	-3.0	8.57	-6.9	6.85	16
Lu	0.273	0.8			0.275	-1.0	0.276	-1.2			1.15	2.2	1.23	-6.5	1.30	-12	1.22	-5.8
Pb	1.50	3.6			1.65	-9.2	1.40	7.2			30.4	0.6	32.6	-6.9	30.8	-1.4	31.5	-3.6
Th	1.19	1.1			1.22	-2.6	1.22	-2.4			32.1	6.4	30.5	5.5	31.0	3.6	31.6	1.7
U	0.423	1.3			0.412	2.7	0.422	0.2			10.6	0.7	10.6	-0.7	10.4	1.5	11.3	-6.6

Diff. %, relative difference (%)
% RSD, Relative standard deviation (%)

GEOSTANDARDS and GEOANALYTICAL RESEARCH

inconsistency for the mass fraction (-24%) and the good repeatability (3.2%) of Ta in JG-2 are likely caused by one or more reasons described above; nugget effect, the difference in the used reference materials and their working values and/or an inappropriate analytical protocol.

To conclude, the mass fractions of IFFEs and HFSEs in the geological reference materials obtained by Method A are regarded as the recommended values in the samples, with the biases in the mass fractions of ± 5% for most (and ± 10% for some) elements compared with the literature data. More importantly, the mass fractions obtained by Method A can serve as the benchmark for evaluating the mass fractions obtained through the simultaneous method because the difference in the used reference materials and their working values are cancelled.

Results of Method B

To evaluate the measurement trueness of the obtained mass fractions of the measurand in rock samples, we compared the mass fractions analysed by Method B with those by Method A using Equation (1):

$$D = \left(\frac{C_{\text{Method B}}}{C_{\text{Method A}}} - 1\right) \times 100 \qquad (1)$$

in which $C_{\text{Method A}}$ and $C_{\text{Method B}}$ are the mass fractions of an element obtained by Method A and B, respectively. Also important to note is that $C_{\text{Method A}}$ for IFFEs and HFSEs in BHVO-2 was determined distinctly by using the samples BHVO-2+Al and BHVO-2, respectively (see the previous section).

Tables 4 and S4 summarise the *D* values and the mass fractions of 27 elements in JB-1a, JB-3, JR-2, JR-2+exMg, JA-2, BHVO-2 and BHVO-2+Al determined using solutions prepared by Method B, respectively. Excellent repeatability (1*s*) of < 3% (< 1% for most elements) was achieved for all IFFEs in the seven samples measured by Method B excluding those of Cs in BHVO-2+Al (9%), Pb in BHVO-2 (14%) and Pb in BHVO-2+Al (12%). The relatively large repeatability may be attributed to the issue of counting statistics; the mass fractions of Cs (0.1 μg g^{-1}) and Pb (1.5 μg g^{-1}) in BHVO-2 are the lowest among those in the other rock samples analysed in this study. The *D* values for most of the IFFEs are generally within ± 5% with some exceptions that exceeded ± 10% (e.g., Cs in JA-2, Lu in JA-2 and Pb in JA-2). Although the reason for these exceptions remains unclear, it should not be associated with the coprecipitation of Cs, Lu and Pb with insoluble fluoride because the other IFFEs would not have coprecipitated with insoluble fluoride.

In most cases, excellent repeatability (within 1–2%, 1*s*) and *D* values (within ± 3–5%) were obtained for HFSEs in the seven samples measured by Method B. However, a problem was encountered with Nb and Ta for JR-2+exMg; the mass fraction of Nb and Ta in JR-2+exMg varied from 28 μg g^{-1} to 171 μg g^{-1} and from 3.5 μg g^{-1} to 18 μg g^{-1}, respectively, across multiple analytical sequences (n = 3), which resulted in significantly large repeatability (> 63%) and *D* values (> 450%).

Results of Method C

To evaluate the performance of Method C in which the samples were decomposed by the high *P–T* digestion system DAB-2, we used Equation (2):

$$D' = \left(\frac{C_{\text{Method C}}}{C_{\text{Method A}}} - 1\right) \times 100 \qquad (2)$$

in which $C_{\text{Method C}}$ is the mass fractions of IFFEs and HFSEs in the samples measured by Method C. The samples tested for Method C were JB-1a, JB-3, JR-2+Mg, JR-2+exMg, JA-1, JA-2, JA-3, BHVO-2, BHVO-2+Al, BHVO-2+exAl, JG-2+Mg and JG-2+exMg. It should be noted that $C_{\text{Method A}}$ for IFFEs and HFSEs in JG-2 was determined distinctly by using the samples JG-2+exMg and JG-2, respectively. The results are shown in Tables 5 and S5.

In this study, except for IFFEs in JA-1, BHVO-2+exAl and JG-2+Mg and HFSEs in BHVO-2, JR-2+exMg, JG-2+Mg and JG-2+exMg, the repeatability and *D*′ values of most IFFEs and HFSEs in all samples analysed through Method C were better than 5% and ± 5%, respectively. Although the repeatability of most IFFEs in JA-1 and BHVO-2+exAl was within 3%, the *D*′ values of most IFFEs for these samples ranged from -13% to +10%. The *D*′ values of Y and most REEs for JA-1 and BHVO-2+exAl were negative, which exceeded the analytical precision of REEs in the same samples measured using Method A (< 2%). The repeatability and *D*′ values of the mass fractions of most IFFEs in JG-2+Mg were > 5% and -34% to +2%, respectively.

The repeatability and *D*′ values for Ti, Zr and Hf in BHVO-2 and JR-2+exMg were less than 2% and within ± 5%, respectively, confirming the validity of Method C for the determination of Ti, Zr and Hf abundances in these samples. The repeatability and the *D*′ values of Nb and Ta abundances in these samples were 5–60% and 15–3000%, respectively. For instance, the mass fraction of Nb in JR-2+exMg varied from 76 μg g^{-1} to 973 μg g^{-1} across the multiple measurement sequences (n = 5), whereas for JR-2

Table 4.
The *D* values of IFFEs and HFSEs in rock samples by Method B (the *D* value is explained in the text)

Sample	JB-1a	JB-3	JR-2	JA-2	BHVO-2	BHVO-2	JR-2
composition	JB-1a	JB-3	JR-2	JA-2	BHVO-2	BHVO-2+Al	JR-2+exMg
(%)	*D*	*D*	*D*	*D*	*D*	*D*	*D*
Ti	0.8	0.4	3.2	0.7	-0.2	-0.6	1.4
Zr	-1.4	-0.1	0.5	4.9	-2.0	-0.8	0.5
Nb	-1.4	0.6	1.7	-0.8	-0.4	-1.1	513
Hf	0.1	0.3	0.5	5.5	-1.7	-1.9	-0.1
Ta	-2.5	-1.0	-2.6	-0.8	-2.0	-1.5	451
Rb	0.0	-0.3	-2.6	4.3	-0.7	-0.7	0.0
Sr	0.9	-0.2	0.0	2.7	-0.1	-1.5	-1.0
Y	0.6	-1.1	-4.5	0.1	0.0	-2.6	2.9
Cs	0.2	0.2	-2.1	9.9	-2.6	6.7	-0.9
Ba	-0.1	-1.8	-1.3	3.3	0.4	0.9	1.4
La	-2.7	-3.1	-5.3	1.5	-2.4	-0.2	0.0
Ce	-1.5	-3.1	-3.3	1.4	-1.4	-0.2	1.1
Pr	0.7	-1.7	0.1	3.2	1.4	0.4	1.7
Nd	1.7	-0.7	1.1	3.7	2.3	0.1	1.6
Sm	1.4	-1.1	0.9	2.1	1.8	0.0	1.3
Eu	1.1	-0.7	0.0	3.4	2.6	0.7	-0.6
Gd	-4.1	-2.2	-4.7	-4.9	-1.2	-0.6	2.1
Tb	2.5	-0.2	2.2	1.5	3.2	-0.9	3.4
Dy	4.2	0.6	3.5	2.5	4.8	-1.0	3.2
Ho	3.9	0.1	3.0	1.5	4.5	-1.1	3.4
Er	4.3	0.4	3.2	2.4	5.4	-0.8	3.1
Tm	4.2	0.1	3.3	2.2	4.7	-1.1	3.5
Yb	4.0	0.6	3.9	2.6	5.2	0.9	3.9
Lu	6.0	8.4	5.6	10.6	5.5	-1.5	2.5
Pb	4.0	5.9	6.7	11.4	8.1	4.1	1.9
Th	4.1	2.1	6.5	6.6	3.7	-0.7	-0.6
U	4.5	1.9	9.1	5.7	3.1	-1.9	-0.5

measured using Method A, the mass fraction was 17.6 ± 0.5 μg g^{-1} (Table 3).

The repeatability of Zr, Hf and Ta in JG-2+Mg and JG-2+exMg was < 5%, whereas their *D*′ values were approximately -10%. However, positive *D*′ values were obtained for Nb in JG-2+Mg and JG-2+exMg (32% and 6.2%, respectively). Moreover, excellent repeatability (< 1%) and *D*′ values (-2%) were obtained for Ti in these samples.

Discussion

Reduction in chemical blanks through Method C

In Method C, we used a stainless jacket made from SUS316Ti, which contains Fe, Ti and trace amounts of Mo, Cr and Ni. Zirconium, Hf, Nb and Ta are also likely to be included in the jacket because they belong to the HFSEs and Ti. The stainless jacket, as well as the PTFE insert in which the sample was digested in acid, could be the source of the chemical blanks. We have evaluated how much the amount of HFSE blanks during high *P–T* digestion can be decreased by repeating the cleaning procedure for the PTFE insert of the digestion system DAB-2. We added a mixture of HF (1 ml) and HPW (1 ml) into the PTFE insert and heated at 225 °C for 48 h; then, the solution was recovered and transferred into a clean PFA vessel. This cleaning step was repeated three times, and the amount of HFSEs in the individual recovered solutions was measured by ICP-MS. The amount of HFSE blanks was determined by the IS method using ^{103}Rh and JB-3 as the internal standard and the reference material, respectively.

The results for the cleaning experiment are shown in Figure 2. The amounts of HFSE blanks decreased from the first to second cleaning step, but remained constant or even increased from the second to the third cleaning step. This result suggests that a single acid cleaning step is effective to minimise the chemical blanks for HFSEs. Therefore, a single-step acid cleaning was performed before sample digestion using the high *P–T* digestion system.

Table 5.
The D' values of IFFEs and HFSEs in rock samples by Method C (the D' value is explained in the text)

Sample	JB-1a	JB-3	JA-2	JA-3	BHVO-2	JR-2	JA-1	BHVO-2	BHVO-2	JR-2	JG-2	JG-2
Composition	JB-1a	JB-3	JA-2	JA-3	BHVO-2+Al	JR-2+Mg	JA-1	BHVO-2+exAl	BHVO-2	JR-2+exMg	JG-2+Mg	JG-2+exMg
(%)	D'	D'	D'	D'	D'	D'	D'	D'	D'	D'	D'	D'
Ti	1.2	-0.1	0.5	0.0	-0.9	1.5	0.6	-0.2	-0.3	4.1	-1.9	-1.3
Zr	-0.3	0.5	5.3	1.4	0.5	6.0	1.5	1.3	0.1	4.2	-13	-8.2
Nb	5.7	-1.2	1.5	-1.0	-1.3	-3.5	1.0	-1.9	24	3054	32	6.2
Hf	1.6	1.1	5.9	1.7	-0.4	3.6	1.1	0.5	0.3	3.7	-13	-8.5
Ta	1.6	-1.1	1.3	-1.6	-1.6	-4.3	1.8	-2.3	15	2790	-12	-8.4
Rb	1.0	0.2	3.6	-0.5	-1.3	-1.0	-0.4	-1.5	-0.1	-1.3	-3.6	-1.4
Sr	2.0	0.2	2.3	-0.4	-1.7	-2.0	-3.1	-1.9	0.5	-1.1	-0.9	-0.2
Y	1.5	-1.2	-0.6	-1.5	-1.0	-3.6	-3.8	-10	1.2	-3.9	-22	4.0
Cs	0.3	1.3	9.6	-0.9	2.1	-1.1	-0.3	5.7	6.2	-1.2	0.7	0.6
Ba	1.1	-1.0	2.9	-2.4	0.7	-1.2	-3.7	0.2	0.7	-1.0	-3.0	-0.8
La	-1.2	-2.8	1.1	-4.3	0.1	-4.2	-13	-7.7	-1.4	-3.8	-34	-0.7
Ce	-0.1	-2.5	1.0	-4.0	-0.1	-0.9	-6.8	-3.0	-0.5	-1.7	-2.6	-0.4
Pr	2.1	-0.7	2.9	-2.0	1.1	-1.0	-9.3	-3.3	1.9	0.4	-27	-0.6
Nd	2.4	0.1	3.6	-0.5	0.6	-0.4	-8.2	-3.5	2.4	0.7	-26	-0.4
Sm	2.1	-0.1	2.3	-1.0	0.9	-1.5	-7.9	-4.9	2.2	0.4	-22	0.1
Eu	2.8	0.3	4.0	0.8	1.4	-1.6	-5.9	-2.7	2.8	-0.5	-24	-0.6
Gd	-2.8	-2.2	-4.9	-4.9	1.0	-3.6	-6.4	-11	-0.6	-4.7	-21	1.5
Tb	3.8	0.7	1.6	0.1	1.3	0.7	-5.3	-6.0	4.0	1.2	-17	-0.7
Dy	4.1	1.6	2.3	1.1	1.7	1.1	-4.4	-4.1	4.9	1.7	-14	0.4
Ho	4.2	0.8	1.7	0.6	1.6	0.5	-4.2	-5.0	4.4	1.6	-12	1.4
Er	4.2	1.1	2.0	1.0	1.5	0.7	-3.5	-4.5	5.2	1.2	-11	1.4
Tm	3.3	1.0	1.9	0.8	1.8	0.8	-3.0	-4.0	4.3	0.7	-11	-0.4
Yb	4.6	1.2	2.2	1.4	3.4	1.5	-2.6	-2.7	5.3	2.1	-11	-1.1
Lu	5.5	9.6	11	8.0	1.9	1.9	2.3	-3.0	5.2	2.8	-12	1.0
Pb	4.5	6.3	11	3.5	4.5	5.0	4.4	10	-2.0	3.5	0.8	1.2
Th	4.1	4.1	6.9	1.8	1.3	0.5	-4.6	-1.2	5.5	2.2	-12	10
U	4.0	3.1	6.0	2.1	-0.3	2.0	-0.7	8.4	4.7	2.6	2.1	5.7

Evaluation of Method B

In Method B, all samples without the addition of Al or Mg solutions showed good D values (within $\pm$ 5%) for most of the determined elements. The Ca-Al-Mg composition of BHVO-2 is out of the acceptable region, where > 95% recovery yields for IFFEs and HFSEs are expected from the previous study. In this study, we obtained precise and accurate mass fraction data for IFFEs and HFSEs in BHVO-2. On the contrary, for Nb and Ta in JR-2+exMg, significantly large D values (> 450%) were obtained. This observation is inconsistent with the result of JR-2 measured by Method A, of which the mass fractions of Nb and Ta were 17.6 $\pm$ 0.5 μg g^{-1} and 2.10 $\pm$ 0.05 μg g^{-1} (Table 3), respectively. We consider that the discrepancy is attributed to the failure of the ID-IS method that used ^{91}Zr and ^{179}Hf as the internal standard elements for the determination of Nb and Ta. During the digestion of Al-poor samples including JR-2+exMg, it is likely that Zr and Hf coprecipitated with insoluble fluorides. The coprecipitation causes the deficiency in the intensity of the internal standard (Z) in Equation (S10) of the Appendix S1, which leads to the erroneous results in Nb and Ta abundances. On the other hand, the isotopic equilibria of Ti, Zr and Hf between the sample and spike have been achieved before coprecipitation of these elements with fluorides, which yielded consistent mass fractions of Ti, Zr and Hf in JR-2+exMg that were determined by the ID method with those of the literature data. JR-2 is a glassy obsidian and easy to dissolve in acid, such that the sample-spike isotopic equilibration was achieved before the reaction of added Mg solution with HF to form insoluble MgF_2 that coprecipitates HFSEs.

The above interpretation is inconsistent with the argument by Tanaka *et al.* (2003) that the coprecipitation of HFSEs with insoluble fluorides did not occur for a sample with Ca# < 0.40 including JR-2+exMg (Figure S1a). The authors argued that adequate recovery yields of HFSEs were achieved for synthetic samples in which the Ca-Al-Mg composition is similar to JR-2+exMg (e.g., Ca:Al:Mg = 0:40:60). Instead, this study showed that HFSEs coprecipitate with Mg-fluorides and Ca-fluorides. For this reason, here we install a parameter Mg#, which is the molar ratio Mg/(Mg+Al), to evaluate the incomplete recovery of HFSEs

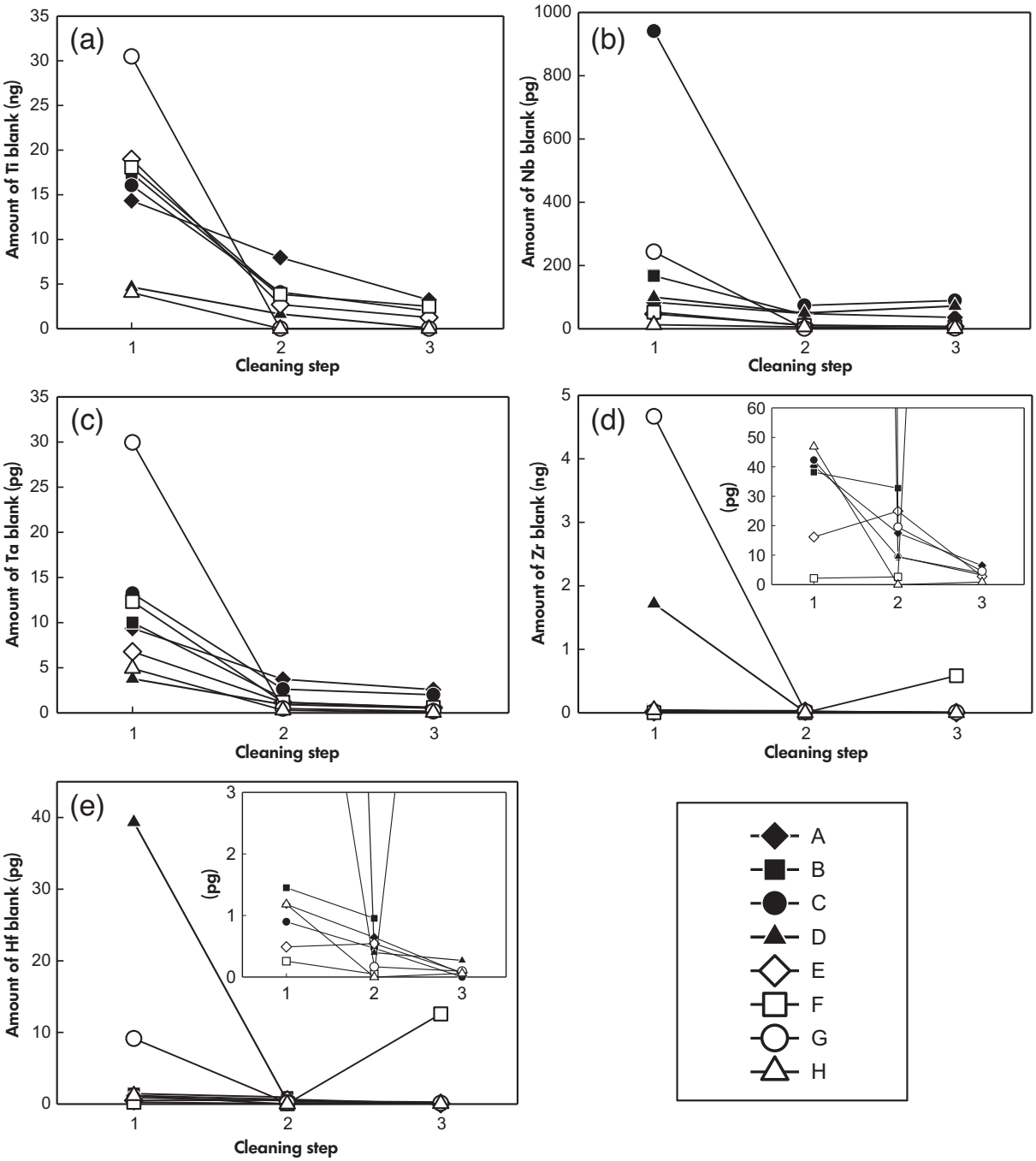

Figure 2. Change in the amounts of chemical blanks for HFSEs by acid cleaning. A–H define different jackets and inserts.

owing to the coprecipitation with Mg-fluorides. To suppress the coprecipitation of HFSEs with Mg-fluorides, Mg# in the sample solution is required to be low. Among the samples examined in this study, BHVO-2 and JR-2+exMg have the highest Mg# (= 0.40 and 0.61, respectively), and the sample showed excellent *D* values (within ± 2%) for all HFSEs. Therefore, Mg# = 0.40 is a conservative criterion that can avoid the loss of HFSEs caused by the coprecipitation with Mg-fluorides. On the other hand, BHVO-2 has the highest Ca# (= 0.43) among the examined seven samples, such that the value can serve as another criterion to avoid the coprecipitation of HFSEs with Ca-fluorides. This condition slightly relaxes the conclusion of Tanaka *et al.* (2003) that Ca# < 0.40 was required to suppress the coprecipitation of

HFSEs with insoluble fluoride, which suggested that the region of HFSE precipitation for an actual rock sample is different from the region proposed previously, in which synthetic samples were used (Figure S1a).

Overall, we confirmed that Method B provides precise mass fraction data for IFFEs and HFSEs in igneous rocks measured in this study. This technique is applicable to samples with Ca-Al-Mg compositions similar to those of JB-1a, JB-3, JR-2, JA-2, BHVO-2 and BHVO-2+Al (Figure 3a). Contrary to an expectation from the previous study, Method B cannot be applied to samples with Ca-Al-Mg compositions similar to those of JR-2+exMg. We conclude that the simultaneous determination of IFFEs and HFSEs by Method B is suitable for samples with Ca# < 0.43 and Mg# < 0.40, that is, the samples with a Ca-Al-Mg composition highlighted in white in Figure 3a. The Ca-Al-Mg compositions of samples plotted in the yellow area of Figure 3a must be adjusted to be within the white area of Figure 3a by Al addition prior to acid digestion.

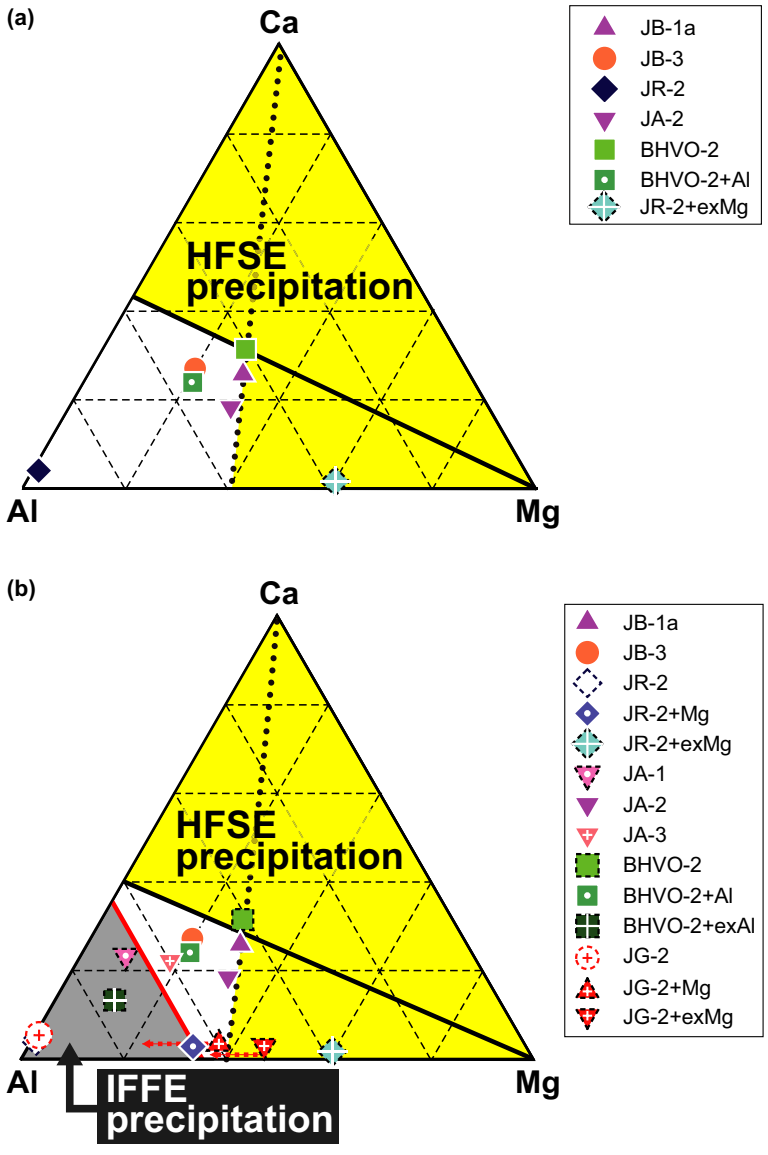

Figure 3. Compositions of samples decomposed by (a) Method B and (b) Method C in this study. Bold black lines indicate Ca# = 0.43 and 0.40 in (a) and (b), respectively. The dotted and red lines are Mg# = 0.40 and Al/(Mg+Ca) = 1.86, respectively. The white areas are regions where samples can be applied to (a) Method B and (b) Method C for the determination of high field-strength elements (HFSEs) and insoluble fluoride-forming elements (IFFEs). See Table S1 for the details of chemical compositions of the measured samples.

Evaluation of Method C

In addition, the measured rock samples were classified into the following three groups: additive-free samples (JB-1a, JB-3, JA-1, JA-2, JA-3 and BHVO-2), Al-added samples (BHVO-2+Al and BHVO-2+exAl) and Mg-added samples (JR-2+Mg, JR-2+exMg, JG-2+Mg and JG-2+exMg).

Additive-free samples: JB-1a, JB-3, JA-1, JA-2 and JA-3 are plotted in the area of Ca# < 0.40 in the Ca-Al-Mg ternary diagram (Figure S1b) where > 95% recovery yields for HFSEs are expected from the previous study. In contrast, BHVO-2 is plotted out of the crosshatched area such that HFSEs in BHVO-2 are considered to coprecipitate with Mg- and Ca-fluorides. Therefore, acceptable D' values (< ± 6%) of HFSEs for JB-1a, JB-3, JA-1, JA-2 and JA-3 and relatively large D' values of Nb and Ta for BHVO-2 (> 15%) are rational.

The D' values of IFFEs in all of the additive-free samples are good (± 5%), while those in JA-1 are systematically negative down to -13%. To evaluate the cause of negative D' values for IFFEs in JA-1, we centrifuged the solutions of JA-1 after acid digestion and determined the mass fractions of IFFEs in the supernatant (Table S6). All of the D' values for the supernatant were lower than those without centrifugation (Figure 4a). This feature is particularly prominent for the elements that form trivalent ions in solution (i.e., Y and REEs), suggesting the coprecipitation of these elements with insoluble fluoride AlF_3 by substituting Al^{3+} site as demonstrated by Takei *et al.* (2001). The authors argued that the samples with Al/(Mg+Ca) > 1.0 were considered to form stable and insoluble AlF_3 during sample digestion under high *P–T* conditions (Figure S1b). However, our results indicate that the insoluble AlF_3 did not form for the additive-free samples with Al/(Mg+Ca) > 1.0 excluding JA-1. This result relaxes the criterion placed by Takei *et al.* (2001); we speculate that the actual condition that can form insoluble AlF_3 through Method C is Al/(Mg+Ca) > 1.50 (JA-3), the value which is the highest among the additive-free samples excluding JA-1.

Al-added samples: The D' values of HFSEs in BHVO-2+Al and BHVO-2+exAl are excellent (< ± 2%) because these samples possess Ca# < 0.40 (Figure S1b). The D' values of IFFEs in BHVO-2+Al are within ± 5%, whereas those in BHVO-2+exAl are all negative values. To investigate the cause of negative D' values for BHVO-2+exAl, the solution of this sample was centrifuged after acid digestion to determine the mass fractions of IFFEs in the supernatant (Table S6). All of the D' values for the supernatant were lower than those in the solution without centrifugation

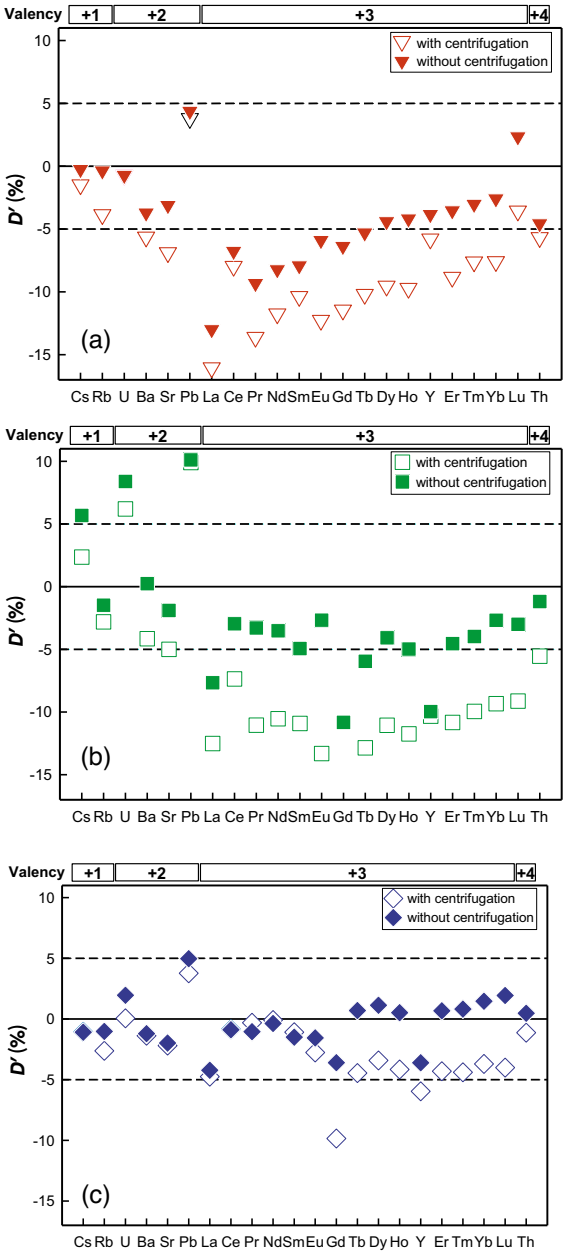

Figure 4. D' values of IFFEs in: (a) JA-1, (b) BHVO-2+exA1 and (c) JR-2+exMg decomposed by Method C. Filled and open symbols represent the data determined without and with centrifugation after acid digestion, respectively.

(Figure 4b), confirming the formation of stable and insoluble AlF_3 that coprecipitated IFFEs. The Ca-Al-Mg composition of BHVO-2+Al is close to that of JB-1a, JB-3, JA-2 and JA-3 on the Ca-Al-Mg ternary diagram (Figure S1b). Here, the formation of insoluble AlF_3 was suppressed, resulting in the acceptable D' values of IFFEs for this sample. In Method C, the simultaneous determination of the mass fractions of IFFEs

and HFSEs in an Al-poor sample (e.g., BHVO-2) is achieved by changing the Ca-Al-Mg composition through the addition of Al solution, thus forming Al/(Mg+Ca) < 1.50 and Ca# < 0.40.

Mg-added samples: The *D'* values for JR-2+Mg are within ± 5% for most of the elements, although JR-2+Mg has a high Al/(Mg+Ca) ratio of 1.86. In such a condition, insoluble AlF_3 is expected to form during high *P–T* digestion as discussed in the previous section. To check the formation of stable and insoluble AlF_3, we centrifuged the solution of JR-2+Mg after acid digestion and determined the mass fractions of IFFEs in the supernatant (Table S6). The *D'* values of Y and heavy REEs (Gd–Lu) in the supernatant of JR-2+Mg are 4–6% lower than those measured without centrifugation (Figure 4c). The systematic decrease in the *D'* values associated with centrifugation suggests the occurrence of insoluble AlF_3 that coprecipitated trivalent ions. Note that the formation of AlF_3 in JR-2+Mg is not particularly problematic if sample solutions are shaken before ICP-MS measurements, as acceptable *D'* values for JR-2+Mg for most elements within ± 5% were obtained. As a result, we surmise that the actual conditions under which insoluble AlF_3 cannot form using Method C are Al/(Mg+Ca) < 1.86 and Ca# < 0.40.

For JR-2+exMg, the large *D'* values (> 2500%) for Nb and Ta and acceptable *D'* values (<± 5%) for Zr and Hf indicate that the isotopic equilibria of Zr and Hf between the sample and spike has been achieved while the ID-IS method for the determination of Nb and Ta failed as a result of coprecipitation of HFSEs with insoluble Mg-fluorides and Ca-fluorides, as is discussed in the previous section (Method B). Therefore, contrary to the previous study, we found that Zr and Hf in samples such as JR-2+exMg were coprecipitated with fluorides after the isotopic equilibria of Zr and Hf isotopes through Method C and Method B.

However, the absolute *D'* values for Zr and Hf, as well as Nb and Ta, are larger than 12% for JG-2+Mg. This observation suggests the failure of isotopic equilibria for Zr and Hf between the sample and spike and then the mass fractions of Zr and Hf, as well as Nb and Ta, are not determined accurately by the ID-IS method in the isotopic disequilibria. We consider that a part of Mg added to the sample was consumed to form MgF_2, where Zr and Hf spikes were incorporated before the DAB-2 digestion. Under high *P–T* conditions, the solution in the DAB-2 insert became Mg-poor (i.e., Al-rich) relative to the expected Ca-Al-Mg composition, resulting in the formation of stable insoluble AlF_3. All of the absolute *D'* values for trivalent IFFEs in JG-2+Mg are < 11%, thus supporting the coprecipitation of these elements with stable and insoluble AlF_3. Compared with JG-2+Mg, the absolute *D'* values for IFFEs are small in JG-2+exMg. Therefore, it is conceivable that the formation of AlF_3 was suppressed in the case of JG-2+exMg as the Ca-Al-Mg composition of the solution in the DAB-2 insert was more Mg-rich in JG-2+exMg than in JG-2+Mg. This conclusion is supported by the fact that the mass fractions of IFFEs in JG-2 determined using Method A, in which a sample with JG-2+exMg composition was decomposed under high *P–T* conditions, were consistent with those of literature.

Unlike JG-2+Mg, isotopic equilibria of Zr and Hf were achieved for JR-2+Mg and JR-2+exMg, as discussed above, although Mg solution was added to these samples. The inconsistency is because of the difference in the petrology of the used samples. JR-2 is glassy obsidian and easily decomposable in acid under standard pressure and temperature. Thus, the expected Ca-Al-Mg composition was achieved in JR-2+Mg and JR-2+exMg under high *P–T* conditions. In addition, the isotopic disequilibria caused by the difference in the dissolution rate of minerals during sample decomposition (e.g., plagioclase, pyroxene and refractory minerals) were discussed by Takei *et al.* (2001).

We obtained excellent *D'* values of Ti (< ± 2%) in all Mg-addition samples and then achieved the isotopic equilibration of Ti between the sample and spike. This result indicates that Ti is not coprecipitated with MgF_2 through Method C, which is consistent with the argument of Lu *et al.* (2007).

Application of Method C: We conclude that the simultaneous determination of IFFEs and HFSEs using Method C is possible for samples with Al/(Mg+Ca) < 1.86, Ca# < 0.40 and Mg# < 0.40, that is, the samples with a Ca-Al-Mg composition highlighted in white in Figure 3b.

For samples with Ca# > 0.40 and Mg# > 0.40, such as BHVO-2 (yellow area in Figure 3b), Method C can be applied if the Ca-Al-Mg composition is adjusted using Al solution before sample digestion. Al addition is effective to avoid the coprecipitation of HFSEs with Ca- and Mg-fluorides. However, an excessive addition of Al in the ratio of Al/(Mg+Ca) > 1.86 causes a problem in the formation of insoluble AlF_3 that coprecipitates IFFEs under high *P–T* conditions.

The mass fractions of IFFEs and HFSEs in samples with Al/(Mg+Ca) > 1.86 are difficult to determine accurately through Method C. The adjustment of the Ca-Al-Mg composition by Mg addition is valid for samples that can

be easily decomposed in acid (e.g., JR-2). The Mg-addition method is difficult to apply to samples containing acid-resistant minerals (e.g., granites) because MgF_2 is formed before sample digestion under high *P–T* conditions. This important finding was overlooked by Tanaka *et al.* (2003), who used synthetic solution samples to determine the compositional range that causes HFSE coprecipitation with fluorides. We speculate that the same problem would occur when Ca solution is added to an Al-rich sample to adjust the Ca-Al-Mg composition because CaF_2 coprecipitates HFSEs.

The problem of fluoride precipitation by Mg (and Ca) addition occurs when both IFFE and HFSE abundances are determined from Method C. The mass fractions of IFFEs in the Al-rich refractory samples can be obtained by the addition of an excessive amount of Mg (e.g., JG-2+exMg). The mass fractions of IFFEs and HFSEs in samples containing refractory minerals with Al/(Mg+Ca) $>$ 1.86 should be determined separately using Method A, on the condition that a large amount of samples are crushed and homogenised to reduce the effect of the sample heterogeneity.

Conclusions

In the present study, we have developed the simultaneous method, in which the mass fractions of IFFEs and HFSEs in rock samples can be determined precisely using a solution prepared by the dissolution of a single sample aliquot and the risk of the incomplete recovery of either IFFEs or HFSEs can be avoided. The performance of the simultaneous method was evaluated by measuring the mass fractions of IFFEs and HFSEs in some geological reference materials and comparing the results with those obtained by the conventional procedure (Method A). Erroneous mass fractions were obtained when either the IFFEs or HFSEs were incorporated into insoluble fluorides that formed during the acid digestion of the samples. To avoid the coprecipitation of IFFEs and HFSEs with fluorides in the simultaneous method, the Ca-Al-Mg composition of the sample must be adjusted to be within the white area of Figure 3 prior to sample digestion with acids. In the case of sample digestion on a hot plate (i.e., Method B), the Ca-Al-Mg composition of the sample must be Ca# $<$ 0.43 and Mg# $<$ 0.40 (Figure 3a). In contrast, when the sample is digested under high *P–T* conditions using DAB-2 (Method C), the allowable range is Al/(Mg+Ca) $<$ 1.86, Ca# $<$ 0.40 and Mg# $<$ 0.40 (Figure 3b). This result is consistent with the notion reported by Makishima *et al.* (2009) that high Al proportion in the dissolved sample is required to determine HFSEs but hinders the determination of IFFEs when the sample is digested using DAB-2. We found that (1) the IFFE and HFSE abundances in a single sample aliquot can be simultaneously determined by the ID and ID-IS methods if the Ca-Al-Mg composition of a sample is adjusted to the specific composition presented above by the addition of Al solution and (2) the addition of Mg (and Ca) solution should not be used for the exchange of the Ca-Al-Mg composition of a sample because MgF_2 and CaF_2 are formed prior to the sample decomposition and adjustment of the Ca-Al-Mg composition.

Although we need to know the compositions of Ca, Al and Mg in the sample solution before applying the simultaneous method, major elements including Ca, Al and Mg are measured by other techniques such as XRF and/or ICP-AES/OES in most cases (e.g., Mittlefehldt *et al.* 2013, Barrat *et al.* 2015). The abundance of major elements can be easily determined by portable XRF although this instrument has lower analytical precision than conventional methods (e.g., XRF and/or ICP-AES/OES) (e.g., Watanabe *et al.* 2020). Therefore, the method presented in this study is used for the simultaneous determination of the IFFE and HFSE abundances with high repeatability (4%) and relatively small biases in the mass fractions of $\pm$ 5% for most of the elements compared to those by the separate methods. The simultaneous method is advantageous in terms of decreasing the requisite amount of a sample in the analysis of multiple elemental abundances and isotopic compositions. This method is specifically beneficial for the analysis of precious materials including asteroid samples returned in space exploration missions (e.g., Hayabusa2 and OSIRIS-REx). In addition, this method is suitable for the determination of IFFEs and HFSEs in heterogeneous samples that contain accessory minerals with extremely high abundances for some IFFEs and/or HFSEs (e.g., zircon, monazite and rutile).

Acknowledgements

We thank M. Nakamura for the technical assistance in the early stage of this research. We are grateful to Prof. Thomas Meisel for editorial handling and the anonymous reviewer for constructive reviews. This research was supported by Grant-in-Aid for JSPS Research Fellow (18J12595) and for Scientific Research (26106002, 26220713, 16H04081, 19H00715 and 20H04609) from the Japan Society for the Promotion of Science. The authors declare no conflict of interests.

Data availability statement

The data that support the findings of this study are available on request from the corresponding author.

References

Awaji S., Nakamura K., Nozaki T. and Kato Y. (2006)
A simple method for precise determination of 23 trace elements in granitic rocks by ICP-MS after lithium tetraborate fusion. Resource Geology, 56, 471–478.

Barrat J.-A., Greenwood R.C., Verchovsky A.B., Gillet P., Bollinger C., Langlade J.A., Liorzou C. and Franchi I.A. (2015)
Crustal differentiation in the early solar system: Clues from the unique achondrite Northwest Africa 7325 (NWA 7325). Geochimica et Cosmochimica Acta, 168, 280–292.

Barrat J.-A., Yamaguchi A., Greenwood R.C., Bohn M., Cotten J., Benoit M. and Franchi I.A. (2007)
The Stannern trend eucrites: Contamination of main group eucritic magmas by crustal partial melts. Geochimica et Cosmochimica Acta, 71, 4108–4124.

Cotta A.J.B. and Enzweiler J. (2012)
Classical and new procedures of whole rock dissolution for trace element determination by ICP-MS. Geostandards and Geoanalytical Research, 36, 27–50.

Dulski P. (2001)
Reference materials for geochemical studies: New analytical data by ICP-MS and critical discussion of reference values. Geostandards Newsletter: The Journal of Geostandards and Geoanalysis, 25, 87–125.

Eggins S.M. (2003)
Laser ablation ICP-MS analysis of geological materials prepared as lithium borate glasses. Geostandards Newsletter: The Journal of Geostandards and Geoanalysis, 27, 147–162.

Eggins S.M., Woodhead J.D., Kinsley L.P.J., Mortimer G.E., Sylvester P., McCulloch M.T., Hergt J.M. and Handler M.R. (1997)
A simple method for the precise determination of ≥ 40 trace elements in geological samples by ICP-MS using enriched isotope internal standardisation. Chemical Geology, 134, 311–326.

Gméling K., Harangi S. and Kasztovszky Z. (2005)
Boron and chlorine concentration of volcanic rocks: An application of prompt gamma activation analysis. Journal of Radioanalytical and Nuclear Chemistry, 265, 201–212.

Heumann K.G. (2004)
Isotope-dilution ICP-MS for trace element determination and speciation: From a reference method to a routine method? Analytical and Bioanalytical Chemistry, 378, 318–329.

Hu Z. and Gao S. (2008)
Upper crustal abundances of trace elements: A revision and update. Chemical Geology, 253, 205–221.

Iida H., Uchida T., Yuchi A., Konishi M., Ito S. and Isoyama H. (2003)
Determination of minor constituents in silicates by an acid digestion/flow injection method. Bunseki Kagaku, 52, 527–532.

Imai N., Terashima S., Itoh S. and Ando A. (1995)
1994 compilation values for GSJ reference samples, "Igneous rock series". Geochemical Journal, 29, 91–95.

Jochum K.P., Stoll B., Herwig K. and Willbold M. (2007)
Validation of LA-ICP-MS trace element analysis of geological glasses using a new solid-state 193 nm Nd:YAG laser and matrix-matched calibration. Journal of Analytical Atomic Spectrometry, 22, 112–121.

Jochum K.P., Weis U., Schwager B., Stoll B., Wilson S.A., Haug G.H., Andreae M.O. and Enzweiler J. (2015)
Reference values following ISO guidelines for frequently requested rock reference materials. Geostandards and Geoanalytical Research, 40, 333–350.

Kamei A. (2016)
Determination of trace element abundances in GSJ reference rock samples using lithium metaborate-lithium tetraborate fused solutions and inductively coupled plasma-mass spectrometry. Geoscience Reports Shimane University, 34, 41–49.

Kon Y. and Hirata T. (2015)
Determination of 10 major and 34 trace elements in 34 GSJ geochemical reference samples using femtosecond laser ablation ICP-MS. Geochemical Journal, 49, 351–375.

Liang Q.I. and Grégoire D.C. (2000)
Determination of trace elements in twenty six Chinese geochemistry reference materials by inductively coupled plasma-mass spectrometry. Geostandards Newsletter: The Journal of Geostandards and Geoanalysis, 24, 51–63.

Liang Q.I., Jing H.U. and Grégoire D.C. (2000)
Determination of trace elements in granites by inductively coupled plasma mass spectrometry. Talanta, 51, 507–513.

Lu Y., Makishima A. and Nakamura E. (2007)
Coprecipitation of Ti, Mo, Sn and Sb with fluorides and application to determination of B, Ti, Zr, Nb, Mo, Sn, Sb, Hf and Ta by ICP-MS. Chemical Geology, 236, 13–26.

Makishima A. and Nakamura E. (2000)
Determination of titanium at μg g^{-1} levels in milligram amounts of silicate materials by isotope dilution high resolution inductively coupled plasma-mass spectrometry with flow injection. Journal of Analytical Atomic Spectrometry, 15, 263–267.

Makishima A. and Nakamura E. (2006)
Determination of major, minor and trace elements in silicate samples by ICP-QMS and ICP-SFMS applying isotope dilution-internal standardisation (ID-IS) and multi-stage internal standardisation. Geostandards and Geoanalytical Research, 30, 245–271.

references

Makishima A., Nakamura E. and Nakano T. (1999)
Determination of zirconium, niobium, hafnium and tantalum at ng g^{-1} levels in geological materials by direct nebulisation of sample HF solution into FI-ICP-MS. Geostandards Newsletter: The Journal of Geostandards and Geoanalysis, 23, 7–20.

Makishima A., Tanaka R. and Nakamura E. (2009)
Precise elemental and isotopic analyses in silicate samples employing ICP-MS: Application of hydrofluoric acid solution and analytical techniques. Analytical Sciences, 25, 1181–1187.

Mittlefehldt D.W., Herrin J.S., Quinn J.E., Mertzman S.A., Cartwright J.A., Mertzman K.R. and Peng Z.X. (2013)
Composition and petrology of HED polymict breccias: The regolith of (4) Vesta. Meteoritics and Planetary Science, 48, 2105–2134.

Münker C., Pfänder J.A., Weyer S., Büchl A., Kleine T. and Mezger K. (2003)
Evolution of planetary cores and the Earth-Moon system from Nb/Ta systematics. Science, 301, 84–87.

Nakayama K. and Nakamura T. (2005)
X-ray fluorescence analysis of rare earth elements in rocks using low dilution glass beads. Analytical Sciences, 21, 815–822.

Orihashi Y. and Hirata T. (2003)
Rapid quantitative analysis of Y and REE abundances in XRF glass bead for selected GSJ reference rock standards using Nd-YAG 266 nm UV laser ablation ICP-MS. Geochemical Journal, 37, 401–412.

Pearce N.J.G., Perkins W.T., Westgate J.A. and Wade S.C. (2011)
Trace-element microanalysis by LA-ICP-MS: The quest for comprehensive chemical characterisation of single, sub-10 μm volcanic glass shards. Quaternary International, 246, 57–81.

Riley T.R., Curtis M.L., Flowerdew M.J. and Whitehouse M.J. (2016)
Evolution of the Antarctic Peninsula lithosphere: Evidence from Mesozoic mafic rocks. Lithos, 244, 59–73.

Sano T., Hasenaka T., Sawahata H. and Fukuoka T. (2006)
Determination of Ti, K, Sm and Gd values in geological survey of Japan reference materials by prompt gamma neutron activation analysis. Geostandards and Geoanalytical Research, 30, 31–37.

Senda R., Kimura J.I. and Chang Q. (2014)
Evaluation of a rapid, effective sample digestion method for trace element analysis of granitoid samples containing acid-resistant minerals: Alkali fusion after acid digestion. Geochemical Journal, 48, 99–103.

Stix J., Gorton M.P. and Fontaine E. (1996)
Major and trace element analysis of fifteen Japanese igneous reference rocks by XRFS and INAA. Geostandards Newsletter, 20, 87–94.

Takei H., Yokoyama T., Makishima A. and Nakamura E. (2001)
Formation and suppression of AlF_3 during HF digestion of rock samples in Teflon bomb for precise trace element analyses by ICP-MS and ID-TIMS. Proceedings of the Japan Academy Series B, 77, 13–17.

Tanaka R., Makishima A., Kitagawa H. and Nakamura E. (2003)
Suppression of Zr, Nb, Hf and Ta coprecipitation in fluoride compounds for determination in Ca-rich materials. Journal of Analytical Atomic Spectrometry, 18, 1458–1463.

Watanabe T., Tsuchiya N., Yamasaki S., Sawai Y., Hosoda N., Nara F.W., Nakamura T. and Komai T. (2020)
A geochemical approach for identifying marine incursions: Implications for tsunami geology on the Pacific coast of northeast Japan. Applied Geochemistry, 118, 104644.

Yokoyama T., Makishima A. and Nakamura E. (1999)
Evaluation of the coprecipitation of incompatible trace elements with fluoride during silicate rock dissolution by acid digestion. Chemical Geology, 157, 175–187.

Yokoyama T., Nagai Y., Hinohara Y. and Mori T. (2017)
Investigating the influence of non-spectral matrix effects in the determination of twenty-two trace elements in rock samples by ICP-QMS. Geostandards and Geoanalytical Research, 41, 221–242.

Supporting information

The following supporting information may be found in the online version of this article:

Table S1. Typical detection limits assuming the sample digestion procedure of 50 mg samples digestion (dilution factor = 4000).

Table S2. Experimental list for samples, condition and the number of runs.

Table S3. Mass fractions of JB-3 reported previously.

Table S4. Mass fraction data of IFFEs and HFSEs in rock samples by Method B and the repeatability of each analysis.

Table S5. Mass fraction data of IFFEs and HFSEs in rock samples by Method C and the repeatability of each analysis.

Table S6. Mass fraction measurement results for IFFE in JA-1, BHVO-2+exAl, and JR-2+Mg decomposed by Method C after centrifugation and the repeatability of each analysis.